# Hexavalent chromium (VI) removal from wastewater by iron impregnated biochar prepared from agricultural waste

**By**

**Waqar Mansoor**

**Registration No. 00000318068**

**Supervisor**

**Dr. Muhammad Ali Inam**

**A thesis submitted in partial fulfillment of the requirement for the degree of Master of Science in Environmental Engineering**

**Institute of Environmental Science & Engineering**

**School of Civil & Environmental Engineering**

**National University of Sciences & Technology**

**Islamabad, Pakistan**

**2023**

# Approval Certificate

Certified that the contents and form of the thesis are entitled.

## "Hexavalent chromium (VI) removal from wastewater by iron impregnated biochar prepared from agricultural waste"

**Submitted by**

**Mr. Waqar Mansoor**

has been found satisfactory for partial fulfillment of the requirements of the degree of Master of Science in Environmental Engineering.

Supervisor: .....

Assistant Professor
Dr. Muhammad Ali Inam
SCEE (IESE), NUST

GEC Member: ……

Dr. Muhammad Arshad
Professor
SCEE (IESE), NUST

GEC Member: ……..……

Dr. Muhammad Hassan
Associate professor
USPCASE, NUST

# Acceptance Certificate

It is certified that the final copy of the MS/MPhil Thesis written by Mr. Waqar Mansoor (Registration No: 00000318068) of SCEE(IESE) has been vetted by the undersigned, found complete in all respects as per NUST Statues/Regulations, is free of plagiarism, errors, and mistakes, and is accepted as partial fulfillment for the award of MS/MPhil degree. It is further certified that necessary amendments as pointed out by GEC members of the scholar have also been incorporated in the said thesis.

Supervisor: ……
Assistant professor
Dr. Muhammad Ali Inam
Dated: …….

Head of Department: …….
Dr. Zeeshan Ali Khan
Dated: …….

Principal & Dean SCEE:……
Dated: ……

# Declaration Certificate

I declare that this research work titled **"Hexavalent chromium (VI) removal from wastewater by iron impregnated biochar prepared from agricultural waste"** is my work. The work has not been presented elsewhere for assessment. The material that has been used from other sources has been properly acknowledged/referred to.

Student Signature:

……

Student Name: Waqar Mansoor

Date: ……

# Plagiarism Certificate

This thesis has been checked for plagiarism. Turnitin endorsed by the supervisor is attached.

Waqar Mansoor
00000318068

Signature: ……

Supervisor: ……

Date: ……

# Dedication

*This research is dedicated to my loving, caring, and industrious Mother and to my sister whose efforts, guidance, and sacrifice have made my dream of having this degree a reality. words cannot adequately express my deep gratitude to them.*

*"O My Sustainer, bestow on my parents your mercy even as they cherished me in my childhood.*

# Acknowledgments

To the highest God be glory in the great things He has done. I acknowledge Your great provisions, protections, and support throughout this course. I am thankful to my supervisor Dr. Muhammad Ali Inam (IESE) for his appreciation, constructive suggestions, criticisms, and encouragement. My deep gratitude goes to him for giving his valuable time in department discussions and concrete suggestions to improve the research work and thesis write-up.

I remain indebted to the committee members, Dr. Muhammad Arshad (IESE) and Dr. Muhammad Hassan (USPCASE) for sparing time from their busy schedules for attending progress reviews and providing their beneficial suggestions and comments in the context of research and thesis.

I also acknowledge Ms. Anisa Tahir (IESE) for all the help he provided during the research work. My appreciation also goes to my parents, family, and class fellows especially Mr. Usama Khalid, and Mr. Usama Jamil, for their efforts, moral support, and suggestions toward my progress in life. I would like to especially thank my best friend Usama Mubashir for being eternal support, trusting in my abilities, and staying with me in all highs and lows throughout this time.

# Contents

# List of Abbreviations

| | |
|---|---|
| RBC | Raw bagasse biochar |
| RBC500 | Bagasse biochar prepared at temperature of 500°C. |
| RBB400 | Bagasse biochar prepared at temperature of 400°C. |
| RBB600 | Bagasse biochar prepared at temperature of 600°C. |
| Fe-BC | Iron modified biochar. |
| MCM-41 | Mobil composition of matter No. 41 |
| MCM-48 | Mobil composition of atter No. 48 |
| EPA | Environmental protection agency |
| WWF | Worldwide fund for nature |

# LIST OF TABLES

# LIST OF FIGURES

# Abstract

Agricultural biowaste derived biochar is carbonaceous material with strong affinity in removing heavy metals from water. Amongst various agro-biomasses, sugarcane bagasse (SCB) has been extensively produced annually i.e., 27 Mega Ton in Pakistan resulting in waste management issues. Moreover, tannery industries are disposing untreated Cr-laden wastewater directly into freshwater bodies. Therefore, in this study, we compare the effectiveness of raw biochar (RBC) and iron-impregnated biochar (Fe-BC) produced from SCB for the removal of hexavalent chromium [Cr (VI)] under different solution chemistries. Moreover, different characterization techniques like Scanning Electron Microscopy-Elemental Data X-ray spectroscopy (SEM-EDX), Fourier Transform Infrared (FT-IR) spectroscopy and Brunauer-Emmett-Teller (BET) was implied to investigate the structural properties of RBC and Fe-BC. The results indicated that (3 g/L) RBC synthesized at pyrolysis temperature of 500°C (RBC500) presented superior Cr (VI) removal performance (73%) when compared with those synthesized at pyrolysis temperatures of 400°C (50%) and 600°C (47%). Therefore, RBC 500 was chemically activated using $FeCl_3$ for further sorption studies. The greater Cr (VI) removal (92.65%) was achieved using 3 g/L Fe-BC at optimum pH (2), contact time (120 min) and initial Chromium (VI) concentration (20 mg/L) when compared with RBC (73.82% Cr (VI) removal). Moreover, Cr (VI) removal performance was influenced under the influence of interfering species and increasing solution temperature. The kinetic study indicated that Cr (VI) sorption by Fe-BC followed Pseudo second order model while Cr (VI) sorption by RBC followed Pseudo first-order model. Freundlich isotherm model presented better fitting of experimental data of Chromium (VI) adsorption using both Fe-BC and RBC. The characterization techniques indicated enhanced surface roughness and metal impregnation onto biochar surface were mainly responsible for excellent Cr (VI) removal in case of Fe-BC when compared with RBC. Furthermore, the FT-IR analysis results revealed that charge neutralization, surface complexation, and ligands exchange reactions were the primary mechanism for the adsorption of Chromium (VI) from aquatic environment. In conclusion, current study provides mechanistic insights into the removal behavior of Cr (VI) species from aqueous streams using indigenous biosorbent material.

Keywords: Biochar, $FeCl_3$ impregnation, Cr (VI) removal, Mechanism, Water treatment

# Chapter 1

# Introduction

## 1.1 Background

Agriculture is the backbone of economy of Pakistan as it gives food security, employment opportunities, and a way to earn foreign exchange reserves. it constitutes 24% of Pakistan's GDP and employs 48% of the labor force(Saeed, MA, Irshad, A, Sattar, 2015). Agricultural waste is the by-product that is produced due to agricultural operations after obtaining the useful products. Agricultural waste includes harvest waste, animal waste, slaughterhouse waste, fertilizers run-off from fields, and even pesticides that enter in air, soil, and water because of agricultural operation (Fahmy et al., 2017). In 2020, 2.42 billion tons of agricultural waste were produced(Fahmy et al., 2017). Pakistan produced 98 million tons in 2020 (Saeed, MA, Irshad, A, Sattar, 2015). Most of it was discarded or incinerated which is a common practice in developing countries but this waste should be managed properly as it presents a hazard to the public health and as well as ecosystem. Managing agricultural waste will not only add value to the respective crop but also provide the raw material for other industries. Agricultural waste can be converted into charcoal, biochar, methanol, ethanol, and biodiesel but can be used for animal feed, composting, and biogas production (EN, S., 2011).

Biomass is abundant and often recognized as the world's greatest source of renewable energy (Farooq et al., 2018). Sugarcane bagasse (SCB) is a major biomass waste produced in many sugarcane industries across the world to produce sugar and alcohol (Government of Pakistan, 2021). Sugarcane is a high-value cash crop in Pakistan, with significant implications for sugar-related sectors. After textiles, the agricultural industry sector is the second largest. Its yield comprises 3.4 percent of agricultural value addition and 0.7 percent of GDP. The crop was grown on 1,165 thousand hectares in 2020-21, a 12.0 percent increase over the previous year's planted area of 1,040 thousand hectares. Production climbed by 22% to 81.009 MT, up from 66.380 MT the previous year (Government of Pakistan, 2021). Approximately 33% of it is obtained as bagasse: a residue that is obtained after crushing and extracting the sugar from sugar cane(Saeed, MA, Irshad, A, Sattar, 2015). Since reuse and recycling methods are highly affected by the chemical configuration and proportion of the material. So, it is essential to take under consideration

the chemical composition of waste material to be reused and recycle (Grigore, 2017a; Grigore, 2017b). Bagasse is fibrous material whose chemical composition varies with place, season, and species. Samples from Egyptian bagasse contain Alpha cellulose made up 43.2%, along with pentosans (21.2%), ash (1.98%), lignin (18.2%), and extractives derived from methanol and benzene (8.3%) (Fahmy et al., 2017). A lot of methods have been established to manage bagasse waste which includes paper, pulp, and board production, raw material for composting, electricity, and heat production, and conversion to a useful product like charcoal or biochar (Fahmy et al., 2017; EN, S., 2011).

Carbon-rich substance called biochar that is obtained by heating the biomass under anaerobic condition at low temperature(X. Guo et al., 2020). biochar is a cheap and environmental-friendly adsorbent that can remove heavy metals (HMs) and organic containment from aqueous medium because of its high specific surface area, nutrient retention capacity, cation exchange capacity, and high oxygen-containing functional group that contains oxygen (Mohan et al., 2014). Biochar when compared with activated carbon, it has a smaller pore size and specific surface area but adsorption capability to adsorb pollutants is approximately equal to activated carbon in respect of hazardous cations and anions(Zhou et al., 2016). However, biochar is anion naturally which can aid the sorption of cations but resists the sorption of negatively charged particle which abundantly found in wastewater(Min et al., 2020a). Several bio-engineering strategies have been established to increase the capacity of biochar to adsorb anions (B. Chen et al., 2011, Z; Wang et al., 2015; R. Li et al.; 2018). Many studies have found that loading a cation on biochar has boosted the removal of anions by biochar (P. Xia et al. 2016; D. Xia et al., 2016).

Chromium is ranked as 24th by abundance present in earth crust and well known carcinogenic (Lunk, 2015).Cr is primarily discharged into the environment from business for example metallurgy, electroplating steel, manufacturing, leather tanning, mining, textile, painting, and dyeing industry, etc. (Yi et al., 2021a; Bayazit & Kerkez, 2014). Chromium shows a widespread oxidation state from -4 to +6. Two states are usually seen in Cr compounds that are trivalent Chromium and hexavalent Chromium (Lunk, 2015). The first one is less soluble and more stable whereas the second one is less stable and more soluble in an aqueous medium (Zhou et al., 2016). Cr (III) is necessary for efficient human metabolism as it accelerates insulin action thus affecting lipids and carbohydrates metabolism (Szydłowski & Łopatyński, 2003). Whereas Cr (VI) is toxic as

much as 500 times when compared to Cr (III) and poses a threat to living creatures through its carcinogenic, mutation, and teratogenesis effect (T. Chen et al., 2015). The USEPA has defined the permissible limit of 0.05mg/L for Cr (VI) in effluent from industries that are being discharged in surface water (Tytłak et al., 2015). In Pakistan, National environmental quality standards have set the highest permitted limit of 0.1mg/L for Cr (VI) in the effluent. Due to the detrimental effect of Cr (VI) on living creatures, it is essential to treat Cr (VI) containing water and reduce its concentration to permissible limits by using economic, environmental-friendly, and sustainable treatment methods. A lot of remediation technique and strategies has been established for Cr treatment for example Reverse osmosis, ultrafiltration, adsorption, chemical precipitation, oxidation/reduction, ion exchange, and membrane separation (Albadarin et al., 2012). Out of all these remediation techniques, adsorption has emerged as a prominent technique because of its cheap cost, selectivity, and simple process (T. Chen et al., 2015; Albadarin et al., 2012). Many studies have found that biochar created through thermochemical method is effective in the elimination of Cr (VI) from an aqueous environment (Dong et al., 2011; Kuppusamy et al., 2016; Shakya & Agarwal, 2019). Also, many studies have revealed that the loading of anion on biochar has increased the elimination affinity of biochar for Cr (Min et al., 2020a; B. Chen et al., 2011; Yi et al., 2021a; F. Ma et al., 2019; B. Wang et al., 2020).

## 1.2 Production and composition of bagasse

Sugarcane is one of four major crops that are harvested in Pakistan which are wheat, rice, maize, and sugarcane. Approximately, 55 MT Sugar-cane is produced annually in Pakistan, and out of 55 MT, 27MT is wasted as residue called bagasse(Saeed, MA, Irshad, A, Sattar, 2015). Bagasse is a fibrous substance that remains after sugarcane is crushed and its sugar is extracted as shown in figure 1. The bagasse has chemical composition which changes from place to place, from season to season and by species. Approximately, Bagasse has a 43% cellulose content. Ash 1.98 percent, pentosans 21.2%, lignin 18.2%, and methanol-benzene extractives 8.3% which is ideal to produce carbon-based biochar (Fahmy et al., 2017).

Figure 1:Sugarcane bagasse

## 1.3 Methods for treatment of bagasse

The following methods have been developed to treat bagasse which includes:

### 1.3.1 Pulp, paper, and board production.

Bagasse pulp from sugarcane is a small in length fiber with little tearing which is same as hardwood pulp. Sugarcane bagasse pulp may almost effectively replace hardwood pulp in almost all types of paper and paperboard. The bleaching chemical bagasse pulp, after being merged with a specific number of long fibers, may be used to produce a range of high-quality culture and domestic papers, for example coated base paper, napkins, double-adhesive paper, high-grade toilet paper, copy paper and so on.

The following steps are followed to make paper from bagasse.

#### 1.3.1.1 Depithing

In this process, the shortest fibers are removed to make biomass of acceptable quality which results in elimination of 30% of it.

#### 1.3.1.2 Chemical pulping and leaching of bleaching.

#### 1.3.1.3 Digestion

Throughout the course of digestion, the fibrous substance is divided into separate pulp fibers, or sclerenchyma cells that are found in bagasse, which are generally 1.0–1.2 mm long.

### 1.3.1.4 Black liquor

In this process, silica present in bagasse is removed to enhance the quality of the paper.

### 1.3.1.5 Bleaching

Pulp bleaching is a process of addition of chemicals in the presence of gas to pulp or secondary chemical to increase its brightness.

### 1.3.1.6 Papermaking

In a paper-making procedure, a suspension of fibers is accumulated one layer at a time and water is allowed to drain through the resulting mat to create a fiber mat. The outcome is a sheet of paper made of flexible fibers layered on top of one another(Rainey & Covey, 2016).

## 1.3.2 Raw material for electricity and heat production

The following steps are involved in producing electricity from bagasse as the raw material. Bagasse is collected as a waste product from sugar refineries and stored in a dry place. To move bagasse from storage to boilers, a railing system is in place. The boilers are massive cylindrical chambers that are divided into two parts: a lower, smaller portion where bagasse is burnt, and a larger part with thick tubes for increased surface area and water tubes nearby. To warm the water that is present in tubes, it was run through an economizer. The water in these tubes will be converted into high-pressure steam after bagasse burning. The steam then flows towards the target through regulated tubes. The methods used to make sugar can benefit from this steam. High-pressure steam is used to power turbines, which in turn causes the generator to rotate. The turbine and generator are connected by a shaft. The generator subsequently generates power, which can then be sold to WAPDA or stored for use by the sugar sector, easing the load of producing electricity. The flow diagram of electricity generation is shown in figure 2.

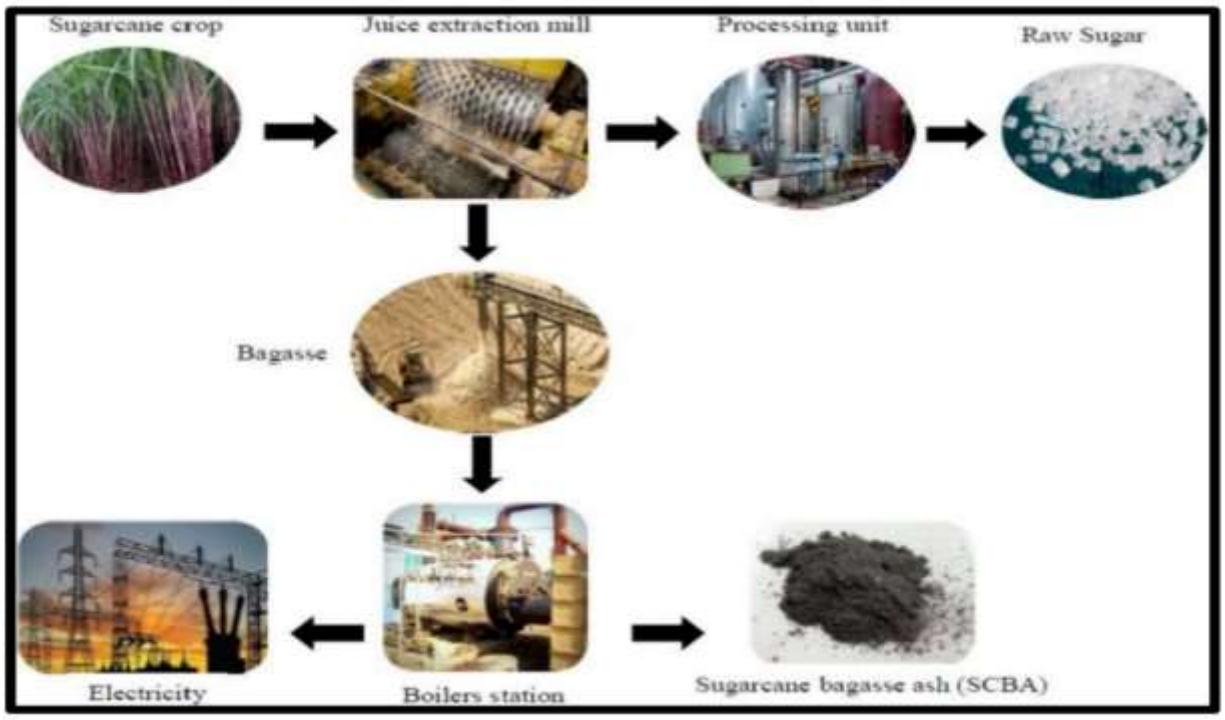


Figure 2: Flow diagram of electricity generation from sugarcane bagasse

### 1.3.3 Conversion to useful products

Biochar (BC) is substance that contain carbon as primary component which is produced when biomass is pyrolyzed at temperatures above 250°C and in low-oxygen (or oxygen-free) environments (O'Connor et al., 2018;Silva et al., 2017). Additionally, because of high carbon present in its composition and high specific surface area (SSA), BC is a viable choice for a number of environmental objectives, along with soil amendment (W. Guo et al., 2019; Joseph et al., 2018; Rizwan et al., 2018; Shaaban et al., 2013). BC has been thoroughly studied for its application for the purpose of adsorbent material for the removal of hazardous components for example heavy metals(HMs), organic and inorganic contaminates present in environment (Bashir et al., 2018; W. Guo et al., 2019; Rizwan et al., 2018; Shen et al., 2018).

## 1.4 Chromium

Chromium is a heavy metal with different character traits depending on its valence states; Cr (III), a trace element, is required by the body, but Cr (VI) is toxic and oxidative (Hayashi et al., 2021).

Chromium and its derivatives are used mostly in metallurgy and pigments. Effluents from these industries are released untreated into rivers, ponds, and seas, where they have a direct impact on living species due to their carcinogenic and mutagenic characteristics. Exposure to heavy metals such as chromium, even at low amounts, is harmful, and its removal remains a difficult issue for current researchers.

### 1.4.1 Sources

Although chromium compounds are only found in minute levels in the water, the element and its compounds can be disposed of in surface water by several industries. Chromium may be found in both natural and man-made environments. Geological natural sources include ultramafic and basaltic rocks, particularly serpentinites; these rocks are commonly replaced by amphiboles, garnets, micas, pyroxenes, and spinel. Tanneries, metal finishing, cooling towers, pigment synthesis, chemical industries and dyeing uses high chromium salts are examples of man-made sources (Kanagaraj & Elango, 2019).

### 1.4.2 Applications

Because of its excellent physicochemical features, chromium oxide ($Cr_2O_3$) has become a prominent research material. Chromium is used to stain glass green and emerald. Cr and its derivatives are utilized as mordants in textile industry, as well as in the aerospace and other sectors to anodize metal. Chromite has been utilized in the refractory sector to make bricks and forms due to its high melting point, mild thermal expansion, and crystalline structural stability. Chromium is used in alloy production, alloy steel preparation to increase corrosion and heat resistance, non-ferrous alloy production to impart unique properties to the alloys, insoluble salt manufacturing and processing, and moth-proofing wool (Babu et al., 2019). An overview of global chromium market is shown in figure 3. Cr3+ and Cr6+ ions can coexist in various ratios in silicate and borate glasses depending on the arrangement of the glass and the melting setting (Mortazavian et al., 2018). Chromium's major purpose in the body is to control blood flow, regulate cholesterol levels, maintain vascular health, boost the immune system, and stimulate protein synthesis (Costa, 2003).

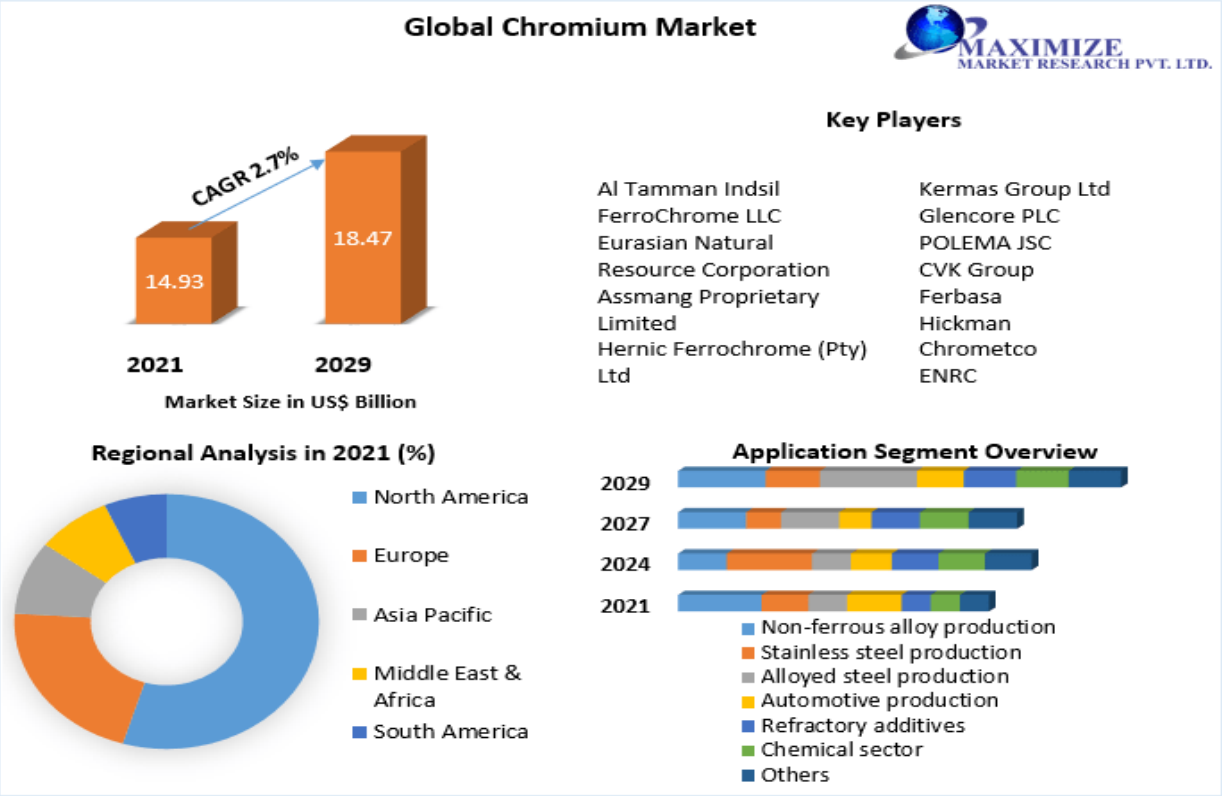


Figure 3: Global chromium market (2022-2029)

### 1.4.3 Effects

Plants require Cr (III), whereas Cr (VI) is hazardous to both plants and animals in low quantities. Because Cr (III) oxides are only partially soluble in water, their concentration is confined in water sources. Cr (VI) compounds are stable under aerobic environments, but under anaerobic conditions, they have converted to Cr (III) compounds. The opposite reaction is also possible in an oxidizing atmosphere. Plants are not harmed by chromium concentrations in soils when it is between 500 to 6000 mg/L (Mohamed et al., 2020). The mechanism of chromium intoxication is pH dependent. As soluble chromates are transformed into insoluble Cr (III) ions, chromium availability to plants decreases. This process protects the food chain from high chromium levels (Sanyal et al., 2015). Cr (VI) is a readily absorbed toxin that may be ingested or breathed. By plundering the respiratory tract, skin contact with Cr (VI) can create vulnerable and genetic abnormalities, as well as cancer (Mohamed et al., 2020). High chromium concentrations in surface water caused by metal product discharge can harm the gills of fish swimming near the disposal site (Wionczyk et al., 2006).

## 1.5 Problem statement

Growing industrialization and urbanization have created a severe danger to groundwater and surface water quality. Groundwater pollution with chromium metal from the tanning and leather industries is a possible environmental and public health problem globally. Chromium occurs naturally as Cr (III) and Cr (VI), with Cr (VI) being more soluble and dangerous than Cr (III). Chromium (VI) can create major health issues, for example lung damage, skin inflammation, and even cancer.

On the other hand, a considerable amount of agricultural waste is burned each year, which has a direct impact upon public health and the ecosystem. Sugarcane is grown in many places in Pakistan, and the excess bagasse is considered trash. To control the surplus of bagasse, proper management is essential. According to a literature review, inadequate handling techniques cause issues and have a detrimental impact on the environment. As a result, its use in the form of biochar through Pyrolysis can be a beneficial process.

Thus, in this research study, biochar was prepared from bagasse and then impregnated with $FeCl_3$ which was called Fe-modified biochar. (Fe-BC). Then a comparative study was done between Raw bagasse biochar (RBC) and Fe-modified biochar (Fe-BC) through different conditions like pH, the different dosages of adsorbate, different initial concentrations, different temperatures, and the influence of the presence of different interfering ions. The different characterization tools like FTIR, BET, and SEM-EDS were used to further explore the comparison of Fe-impregnated biochar (Fe-BC and RBC). Additionally, the regeneration and recycling of Fe-Impregnated biochar (Fe-BC) were also investigated.

## 1.6 Research objectives

The primary goal of this research project is as follows:

- Preparation, modification, and characterization of biochar obtained from sugarcane bagasse through slow pyrolysis process.
- Influence of water chemistry parameters and conditions on the adsorption performance of biochar towards Cr (VI) species
- Exploring the Cr (VI) elimination mechanism using mathematical models and analytical techniques

# Chapter 2

# Literature Review

## 2.1 Background

Environmental contamination is one of the main problems with which the whole world is dealing including Pakistan. This issue is being faced by many nations, including Pakistan, because of population growth, the consumption of natural and manmade resources, industrialization, and excessive reliance on fossil fuels. Every part of our lives in some way affects the quality of the air, the water, or the soil. Water contamination is largely caused by rapid industrialization.

Water is regarded as a resource that is expandable and is therefore a necessity for supporting life and the environment. Over eight billion people worldwide are currently experiencing a severe water shortage. Pakistan has a water shortage having only 930 $m^3$ of water accessible per person per year. The country's water resources are being rapidly depleted due to rapid industrialization, urbanization, and rising irrigation demands for agriculture. This harms agricultural productivity and population health (WWF, 2021). Rivers, lakes, and freshwater underground reservoirs are all contaminated by the wastewater that was released. The water is consequently unfit for home use.

Due to their adverse effects both for aquatic flora and fauna and humans, toxic metals in the environment are a worldwide problem. Although heavy metals cannot decompose, dumping them into soil and water poses serious environmental threats (Agrafioti et al 2014). Among the most hazardous heavy metals include arsenic (X. Sun et al., 2021), lead (Das et al., 2021), and chromium (T. Li et al., 2021). Researchers from all over the world are focusing on eradicating or reducing the concentration of these heavy metals present in wastewater to acceptable levels.

## 2.2 Chromium removal technologies

Chromium removal technologies include (Karimi-Maleh et al., 2021)

- Electrocoagulation
- Ion exchange
- Photocatalysts
- Membrane technology

- Adsorption

### 2.2.1 Electrocoagulation

Particularly, the efficient and effective processes for eliminating pollutants from water is electrocoagulation that involved running an electric current through metal plates to remove fine particles and contaminants and reverse the electric charge that is present on contaminants, causing them to agglomerate (Nidheesh et al., 2021). Genawi et al. (2020) studied the removal of Cr (VI) present in the real wastewater discharged from tannery industry using electrochemical cell with iron electrode. They studied and optimized the operating parameters such as initial Cr (VI) concentration, current density, pH, and power consumption. They achieved 100% Cr (VI) removal at current density of 13mA/cm$^2$, pH at 7 and initial concentration of 750 ppm (Genawi et al., 2020). For limited wastewater with low temperature and turbidity, and flocks that are produced in this process are stable and resistant to acid as compared to that are produced in chemical coagulation; yet, when aluminum or aluminum sulfates are utilized in electrocoagulation, its efficiency for Cr (VI) has increased three times (Golder et al., 2007). Although, Electrocoagulation has performed well in wastewater treatment but sludge formation, high energy consumption, toxic intermediaries of process are the disadvantages of this wastewater treatment technology (Akhter et al., 2022).

### 2.2.2 Ion exchange

Another efficient and prominent physicochemical process is ion exchange that involves the exchange of ions between solids and liquids (Hu et al., 2020) and has had great results in removing Cr (VI). Several ion exchange resins have been developed to eliminate Cr (VI) from water. The matrix of commonly used ion exchange resins is a three-dimensional molecular network with chemically bound charged functional groups. Sapari et al. (1996) used synthetic ion exchange resin (Dowex 2-X4) to obtain 100% removal of Cr (VI) for wastewater from plating industry (Sapari et al., 1996). Amberlite™ IRN77 and SKN1 cation resins show good results and remove 95% Cr (VI) from water. IRN77 and SKN1 displayed adsorption capacities of 35.38 and 46.34 mg/g, correspondingly (Rengaraj et al., 2001). The resin dosage, pH of solution, and original Cr (VI) concentration are all crucial elements for the ion exchange process (Fu et al., 2013).

The primary disadvantages of this procedure include competition with competing ions, such as sulfate, carbonate, and phosphate, reduce elimination efficiency. The other disadvantage is that the procedure is costly due to the costs of resin, waste removal, and regeneration.

### 2.2.3 Photocatalysts

Another extremely successful and cost-efficient technique for the reduction of Cr (VI) is photocatalysts, which emit no hazardous compounds (Farooqi et al., 2021). Attempts have been made to discover a very effective photocatalyst to reduce the Cr (VI) to Cr (III) when exposed to UV radiation, solar energy, and especially visible light (Liu et al., 2020). Some photocatalysts used for this purpose include $WO_3$, $SnS_2$, CdS, CuS, and $Ag_2S$, however, they are limited by slower reduction rates and low efficiency (Niu et al., 2020). Jamaluddin et al., 2022 studied the removal of Cr (VI) by adsorption assisted photocatalyst which showed 28.9% more removal efficiency than conventional adsorption technique.

### 2.2.4 Membrane technology

Membrane filtration is another well-known wastewater treatment method.(Tanhaei et al., 2014) and it is used to eliminate Cr (VI) from wastewater (Adam et al., 2018).Various membranes, depending on pore size, are used for this purpose, including:

- Microfiltration
- Ultrafiltration
- Nano filtration
- Reverse Osmosis

#### 2.2.4.1 Microfiltration (MF)

Since Cr (VI) ions are smaller in size, they are difficult to separate by microfiltration or ultrafiltration. As a result, a chemical change is required to flocculate Cr (VI) ions with the other large molecules and compounds present(Doke & Yadav, 2014). Doke and Yadav (2014) employed a method which has surfactant-based membrane with cetylpyridinium chloride as a cationic surfactant called micellar-enhanced microfiltration (MEMF). They found out that titania membranes can be used effectively for the removal of Cr (VI) from the wastewater.

#### 2.2.4.2 Ultrafiltration (UF)

One of the membrane technologies that use the least amount of pressure is ultrafiltration (UF). The main use of UF is the separation of contaminants with a high molecular weight, such as peptides and polysaccharides. UF membranes cannot separate ionic species because of their limited pore size (Yoon et al., 2009). Basumatary et al. (2016) used MCM-48, MCM-41, and FAU zeolite put over UF membranes with porous ceramic support to examine the removal of Cr (VI) in

crossflow mode ultrafiltration. FAU, MCM-41, and MCM-48 membranes have removal efficiencies of 82%, 75%, and 77%, respectively. Polymer-enhanced ultrafiltration (PEUF) (Haktanır et al., 2017) and micellar-enhanced ultrafiltration (MEUF) (Elfeky et al., 2017) membranes are also utilized for the elimination of Cr (VI).

### 2.2.4.3 Nanofiltration (NF)

In addition, nanofiltration is being utilized to achieve permissible limits of Cr (VI) for wastewater (Wei et al., 2019). NF300 membrane outperformed the PN400 nanofiltration membrane in terms of removal efficiency, removing 97% of Cr (VI) from dual medium, respectively(Gaikwad & Balomajumder, 2017). It was discovered by them that as pressure increased, so did the removal efficiency of Cr (VI) and that this removal efficiency would reduce as feed concentration increased. Bohdziewicz et al. (2000) studied the elimination of Cr (VI) utilizing an NF membrane with a thin coating of charge, the surface of which hinders the combination of Cr and other negative surface particle that are anions (Bohdziewicz, 2000). As pH climbed by 10, the data revealed a rising trend. This is because membrane surface deprotonation enhanced electrostatic repulsion and $CrO_4^{-2}$ formation.

### 2.2.4.4 Reverse osmosis

The reverse membrane (RO) method is useful for removing Cr (VI). To obtain the maximum effluent water purity, RO membranes are operated at high pressures. Cr (VI) present in an aqueous medium using polyamide RO membranes are removed by Gaikwad and Balomajumder (2017) (Gaikwad & Balomajumder, 2017). Increasing the pressure and reducing the concentration of Cr (VI) in the feed boosted their removal, according to the results. When the pH of the solution environment was elevated to 8, elimination of contaminants increased as well.

A schematic diagram of membrane filtration is shown in figure 4. Since some of the membrane technologies has the capacity to remove Cr (VI) from wastewater and surface water but these technologies have high capital and operational cost.

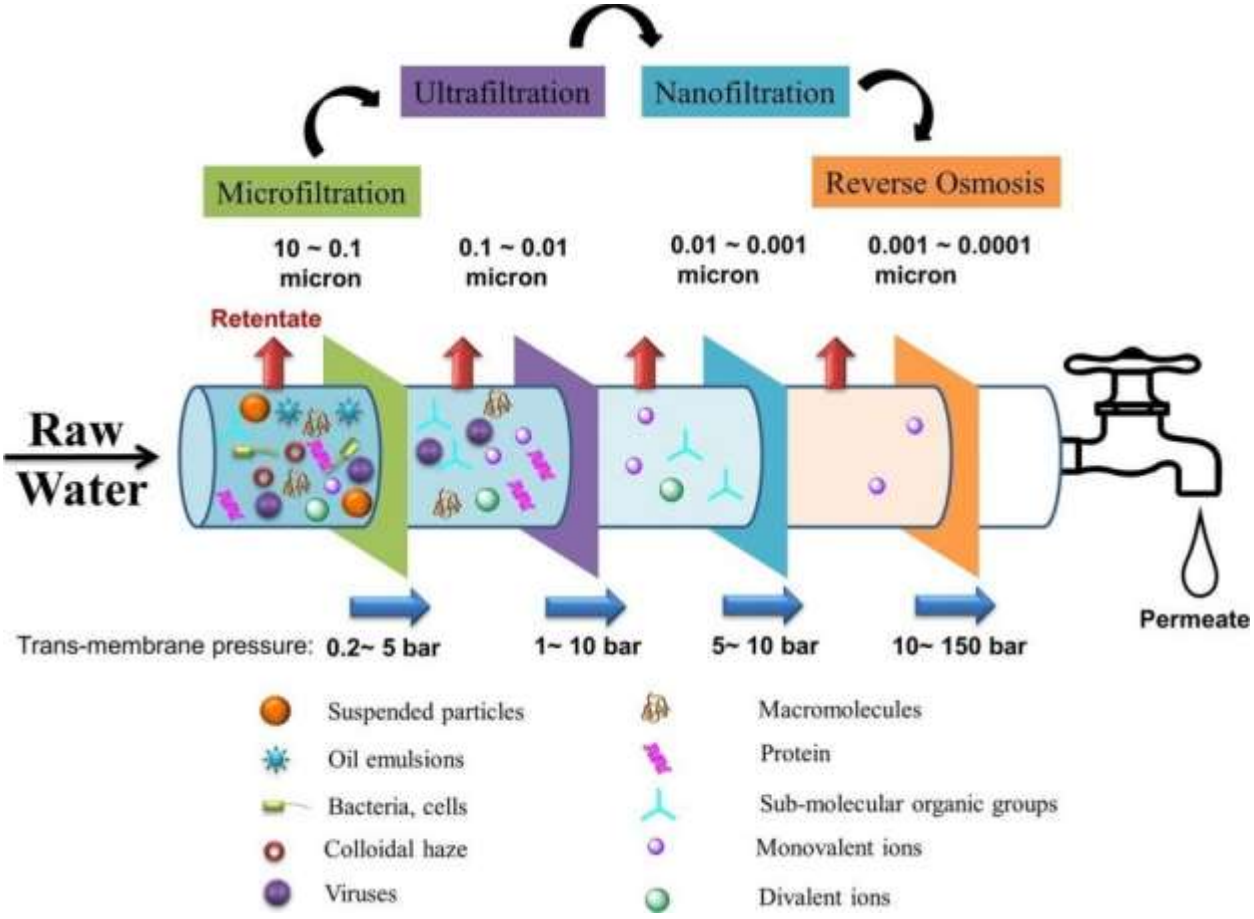


Figure 4: Schematic representation of membrane filtration

### 2.2.5 Adsorption

Heavy metals (HMs) like Cr (VI) can be removed by adsorption which is a suitable, competent, and adaptable method (Yaashikaa et al., 2019). For elimination of Cr (VI) from contaminated water, researchers have been seeking appropriate adsorbents with greater removal capacity and adsorption ability. A range of adsorbents, including natural organic, natural inorganic, and synthetic adsorbents, have been studied for this purpose (Pakade et al., 2019). These adsorbents have been employed in their original form, but their modification, which includes changes in chemical structure, cross-linking, and grafting, has piqued the interest of many researchers. Four mechanisms for the interaction of Cr (VI) with adsorbents are described by Pakade at el., 2019 (Pakade et al., 2019) as follows:

- Adsorption through electrostatic forces
- Cr (VI) to Cr (III) reduction

- Ion Exchange mechanism
- Complex formation

### 2.5.5.1 Features of ideal adsorbent

The size of the particles of adsorbent material is most important for improving adsorption removal performance (Hamadi et al., 2001). The essential properties of an effective adsorbent are followed as below as described by (Bhatnagar & Minocha, 2006).

- The adsorbent has pore structure of uniform of size.
- Adsorbent possesses a high volume of surface area.
- It requires less time to achieve reaction equilibrium.
- It possesses a high level of chemical and physical strength.

## 2.5.6 Adsorbents for the elimination of Cr (VI)

Adsorbents that are often implied for elimination of Cr (VI) include.

- Activated Carbon (AC)
- Graphene Oxide
- Biochar

### 2.5.6.1 Activated carbon

Because of their diversity, activated carbons are frequently used as adsorbents. Their characteristics may be changed to meet specific needs. The most essential characteristics of activated carbon are their large pore volume and specific surface area, which maximize interaction between adsorbent and effluent for optimal removal efficiency. The biggest drawback of activated carbon is their high production cost (Danish & Ahmad, 2018). The results revealed that the activated carbon produced from fox nutshell has a large surface area, the overall process is endothermic, and the greatest adsorption capacity determined to be at pH 2 (Kumar & Jena, 2017).

### 2.5.6.2 Graphene oxide

Graphene is a single-atom-film of covalently linked atoms of carbon in a two-dimensional honeycomb crystal lattice (Yang et al., 2010). It exhibits specific electrical, thermal, and mechanical characteristics, such as improved charge carrier mobility and thermal conductivity, and has therefore been employed in sensors, supercapacitors, batteries, catalysts, and field-effect transistors (Zhang et al., 2013). But treating wastewater with graphene-based adsorbents remains

a difficulty. Ma et al. 2020 produced a graphene adsorbent containing an amine group (ED- RGO) from graphene oxide and discovered that the removal of Cr (VI) by adsorbent was better whereas the solution pH was less than 2 (H.-L. Ma et al., 2012)

### 2.5.6.3 Biochar

Biochar is often made from organic materials such as agricultural and industrial waste, municipal rubbish, and algal biomass. Because of its effective adsorption characteristics for a different contaminant, it is considered a useful adsorbent material. Potential uses of biochar are shown in figure 5. Functional groups present on the surface of the biochar, for example lactones, phenolic hydroxyls, carboxylic acids, carbonyls, quinone, ethers, and condensed aromatic rings, presenting active position for metal adsorption (Herath et al., 2021b). Additionally, adopting agricultural waste as a source for biochar production is compatible with the idea of sustainable development and green economy. Extensive research has been done to explore the removal of heavy metal by biochar using adsorption. Ai et al. (2019) discovered that adsorption affinity of Cr (VI) by sugar beet tailing biochar under acidic conditions achieved 123 mg/g (Ai et al., 2019). Corn cobs hydro char treated with polyethylene amine enhanced the efficiency of Cr (VI) elimination, and the maximum adsorption capacity is 33.66 mg/g (Shi et al., 2020). A surge has been recorded in biochar activation in recent years, and two approaches have been widely adopted to produce porous structures to increase adsorption performance.

- Physical Activation
- Chemical activation

### 2.5.6.3.1 Physical activation

Biochar is typically activated physically at 900°C using steam or $CO_2$.(Qu et al., 2021) Carbonizing feedstock is followed by activating the resultant biochar at high temperatures with appropriate oxidizing gases, such as carbon dioxide, steam, air, or sometimes both gases together (Di Stasi et al., 2019). The activation temperature lies in the range of 600°C and 900°C, while the carbonization temperature is between 400$^{o}$C and 850$^{o}$C, with temperatures surpassing 1000$^{o}$C on occasion. Physically activated carbon lacks the necessary characteristics to be used as an adsorbent or filter (Ioannidou & Zabaniotou, 2007).

### 2.5.6.3.2 Chemical activation

Chemical activation has received more attention than physical activation due to its more cost-effective working conditions and greater product attributes for example increased specific surface area and as well as increased porosity (Aghababaei et al., 2017). The primary con of chemical activation is corrosivity of the apparatus. Furthermore, after activation, the obtained adsorbent must be rinsed with a suitable solvent to remove the excessive activating agent (Ioannidou & Zabaniotou, 2007). Chemical activators often applied include $ZnCl_2$, KOH, $H_3PO_4$, $FeCl_3$, and $K_2CO_3$. Biochar synthesis and activation might be accomplished in a single or two-step process. The feedstock is combined with the activating agent before being pyrolyzed in a single process at a sufficient temperature. In a two-step method, biochar is synthesized in the first stage and then treated with the agent in the second. However, because of better surface characteristics of the adsorbent produced using former technique, the two-step procedure has been regarded as preferable to the one-step technique (Abbaci et al., 2022).

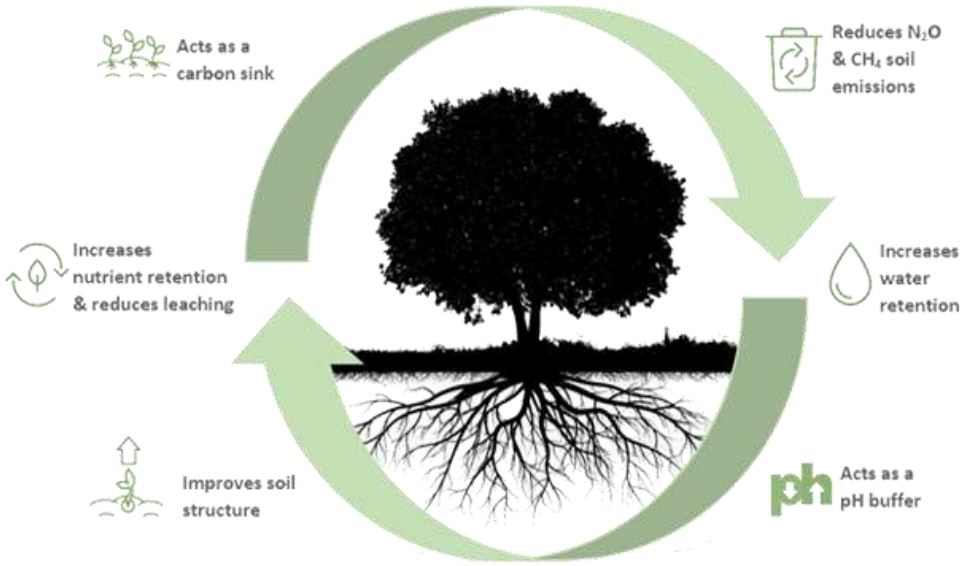


Figure 5: Uses of biochar

# Chapter 3

# Material and Methods

## 3.1 Feedstock preparation

SCB used to produce BC was obtained from local sugarcane juice shop in Rawalpindi, Pakistan. Firstly, the SCB was washed to eliminate the dirt and other impurities and then sun-dried. Secondly, the sun-dried SCB was crushed to convert into powder form using an electric grinder to achieve a particle size of 0.25mm-2mm.

## 3.2 Experimental setup and pyrolysis procedure

Figure 6 depicts different components of the experimental setup that was used to produce biochar. The setup includes:

- Fixed Bed reactor
- Heater
- PID temperature controller
- Flow meter for Nitrogen
- Condenser
- Nitrogen cylinder
- Thermocouples

The fixed bed reactor was prepared from stainless steel which has dimensions of 20 inches. The external and internal diameter of the reactor is approximately 4 and 4.5 inches respectively. The heater is attached outside the reactor to approach the temperature of 1000°C at the rate of 20 °C / minute. PID temperature control and thermocouple are there to control the temperature of the reactor. A flow meter and nitrogen cylinder are used to store and regulate the flow of nitrogen. Condenser was used to condense the heated gas that came out of the reactor to obtain the liquid for further studies.

For biochar preparation, 100 g of biochar was fed into a fixed bed reactor. Before turning on the heater, $N_2$ was introduced into the reactor at the rate of 600 ml per minute to achieve an oxygen-free environment. The purging of nitrogen was done for 30 minutes After 30 minutes, the heater

was turned on and the purging rate decreased to 50 ml/min. Biochar was prepared at three different temperatures of 400 °C, 500 °C, and 600 °C. The desired temperature was achieved by increasing temperature at a rate of 20 °C/min and maintained for 2 hrs. Afterwards, the heating is turned off. A condenser was attached to the reactor to condensable gases to obtain bio-oils. The biochar was obtained from the reactor after it was cooled. The obtained biochar was stored in airtight bags for further use.

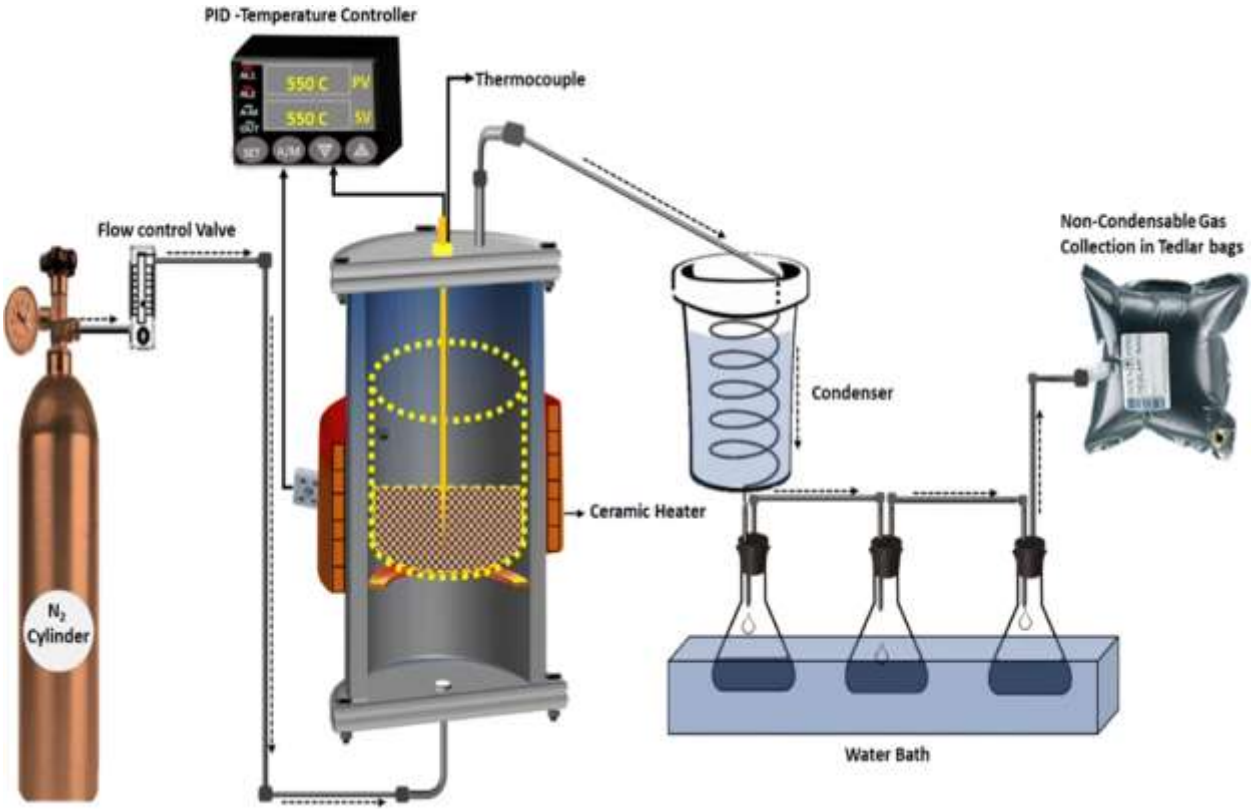


Figure 6: The schematic diagram of the experimental setup

## 3.3 Biochar selection and modification

After the production of BC at three different temperatures, Cr (VI) removal experiments were performed. the BC performed better and was selected for modification that was biochar obtained at 500°C. For modification of BC, 1000 mL of 0.1 Molar $FeCl_3$ solution was processed and prepared. 10 grams of RBC was added into this solution and stirred for 45 minutes. The pH of the suspension was changed to 11 by addition of NaOH pallets with continuous stirring. After 45 minutes, the suspension was then filtered, and the filtrate was washed several times with DI water

to normalize its pH (7-8). Finally, the washed filtrate was put in the oven at 70$^{o}$C for 24 hours. The modified BC was named Fe-BC.

## 3.4 Characterization of biochar and Fe-biochar

A variety of analytical methods were used to analyze raw biochar and Fe-impregnated biochar to evaluate the effect of chemical addition with biochar. The section that follows provides the experimental process as well as some theoretical background for each technique.

### 3.4.1 Proximate analysis

For proximate analysis, raw and Fe-modified biochar were examined using ASTM standards D3175, D3174 and D3173 for ash content, fixed carbon, volatile matter, and moisture content respectively. To evaluate moisture content, measured samples were heated for 24 hours at 105°C degrees Celsius. After oven drying, samples were taken from the oven and the change in weight was used to calculate the moisture content. Volatile matter samples were put in crucibles with covers and put in a muffle furnace and heated at 950 °C for 7 minutes. After the time was over, samples were obtained, and the difference in weight of the samples revealed volatile materials. For ash content tests, crucibles having samples covered with lids were put in a muffle furnace at 725°C for 3 hours.

### 3.4.2 BET analysis

The surface area & pore size analyzer was used to calculate the Surface textural parameters of all adsorbents at a temperature of 77K. (NOVA 2200e, Quanta-chrome Instruments). All the adsorbents were degassed overnight to eliminate moisture before the testing. The temperature for degassing was set at 150 °C. The BET surface area was calculated using the multipoint technique (SBET). Isotherms for all adsorbents were plotted between relative pressure p/po = 0.99 and quantity of $N_2$ adsorbed in $cm^3/g$. pore volume was measured by calculating the amount of Nitrogen absorbed at relative pressure p/po = 0.99. Average pore width was measured using data from density functional theory (DFT) approach, and the pore width was plotted versus the amount of $N_2$ absorbed in $cm^3$ /g.

### 3.4.3 SEM-EDS analysis

SEM and energy dispersive spectroscopy were applied to examine surface morphology of raw and activated samples (51-ADD007, Oxfords Instruments). The voltage of acceleration was

adjusted at 20 kV to capture the SEM pictures. And various magnifications, such as 10X, 100X, and 1000X, were employed.

### 3.4.4 Fourier infrared spectroscopy (FTIR)

Fourier infrared spectroscopy was implied to identify the functional groups present on the surface of adsorbents (FTIR; Bruker Spectrum 400 spectrometer). The KBr disc approach was employed for this purpose with a wavenumber between the range of 4000 to 400 $cm^{-1}$ and a resolution of 1 $cm^{-1}$

### 3.4.5 Point of zero charge (PZC)

The adsorbent's Point of Zero Charge (PZC) was calculated using the approach used by (Godinho et al., 2017; Mortazavian et al., 2018). In each flask, 0.1 g of adsorbent was blended with 50 mL of 0.1 Molar solution of NaCl. The NaCl solutions' pH was initially changed to 3, 4, 5, 6, 7, 8, and 9 by using 0.1 Molar HCl or 0.1 Molar NaOH. The samples were shaken for 24 hours, following which the concluding pH of the samples were measured using a pH 700, pH/mV/°C/°F meter. A plot between initial pH against pH at equilibrium was used to calculate the PZC.

## 3.5 Adsorption experiments

To make stock solution of Cr (VI) of concentration (1000 mg/L), 2.82g of potassium dichromate ($K_2Cr_2O_7$) was dissolved in 1000 ml of distilled water.

### 3.5.1 Selection of efficient adsorbent

Adsorption studies were performed to choose the most effective adsorbent by stirring 0.3 g of adsorbent biochar in 100 mL Cr (VI) solution at 200 rpm. Initial Cr (VI) value was 20 mg/100 ml. The concluding concentration of Cr (VI) was evaluated by UV-Spectrometer after filtering (Specord 200 plus Germany). The adsorbent's removal percentage (%) and adsorption capacity (mg/g) was determined as follows.

$$R\ (\%) = \frac{C_o - C_f}{C_o} * 100$$

$$q_e \left(\frac{mg}{g}\right) = (C_o - C_f) * \frac{V}{m}$$

where $C_o$ (mg/L) and $C_f$ (mg/L) are the starting and final Cr (VI) concentration, respectively. V(L) represents the volume of the solution, and m represents mass of the absorbent.

Following the selection of an effective adsorbent, batch tests were performed to improve the experimental parameters, which included adsorbent dose, pH, contact duration, starting concentration, and temperature.

### 3.5.2 Experimental parameter optimization

To optimize the experimental set-up for the adsorption of Cr (VI), each parameter was modified one at a time while the others remained constant.

The influence of the adsorbent dosage was explored by adjusting it from 0.1 to 0.5 g/L. Other parameters include an initial Cr (VI) concentration of 100 mg/L, a pH of 2, a contact duration of 120 minutes, a temperature of 25°C, and an RPM of 200.

The influence of pH was explored by altering the pH value in the range of 2-10. Other parameters include an initial concentration of Cr (VI) of 100 mg/L, an adsorbent dosage of 3 g/L, a contact period of 120 minutes,25°C temperature, and a 200RPM rotational speed.

The effect of contact duration varied from 0 to 180 minutes, with samples tested at various time duration (10, 20, 30, 40, 50, 60, 70, 80, 90, 100, 110, 120, 130, 140, 150, 160, 170, 180 minutes). Other criteria are the starting Cr (VI) concentration of 20 mg/L, dose of adsorbent 3g/L, pH 2, temperature 25°C, and RPM 200.

### 3.5.3 Adsorption kinetic studies

Two well-known kinetic models, the Pseudo-first order (PFO) kinetic model and the Pseudo-second order (PSO) kinetic model, were employed to quantify the adsorption of Cr (VI) by the adsorbent.

$$q_t = q_e * (1 - e^{-k_1 t})$$

$$q_t = \frac{q_{e^2} * k_2 * t}{1 + q_e * k_2 * 2}$$

where $q_e$ (mg/g) shows the concentration of Cr (VI) absorbed at equilibrium and $q_t$ (mg/g) represents the concentration of Cr (VI) absorbed at time 't'. K1 (minWWW$^{-1}$) and k2 (g/mg/min) are the rate constants.

## 3.6 Adsorption isotherm studies

To quantify the adsorption data, two prominent isotherm models, namely the Langmuir Isotherm model and the Freundlich Isotherm model, were implied. These models predict both single and multilayer adsorption.

$$q_e = \frac{q_{max} * k_L * C_e}{1 + k_L * C_e}$$

$$q_e = k_F * C_e 1/nF$$

where $q_{max}$ (mg/g) represents the adsorbate absorption capacity onto the adsorbent. $K_L$ is the energy constant, 1/nF represents sorption intensity coefficient, and $K_F$ is the adsorption capacity (mg/g) coefficient.

## 3.7 Reusability test

Reusability experiments of adsorbent material were also performed to identify the employed adsorbent's removal effectiveness and adsorption capacity. The procedure for the regeneration of the absorbent was followed as described. The Cr (VI) loaded biochar was collected after filtration and stirred for 12 hours in 1Molar NaOH solution for desorption purposes. After stirring for 12 hours. After that the sample was filtered and washed several times to neutralize pH. The washed sample was put in an oven at 105$^{o}$C for 24 hours for drying purposes. The reusability experiments were performed several times.

## 3.8 Effect of interfering ions

Several interfering ions i.e., $CaCO_3$, $Na_2PO_4.12H_2O$, $Na_2SO_4$, $MgCl_2$, and Humic acid along with Cr (VI) were also tested to investigate their effect on the elimination percentage of Cr (VI). The adsorbent dosage of biochar for these experiments was 3g/L and the contact time was 2 hours. The concentration of these interfering ions was 20 mg/L.

# Chapter 4

# Results and Discussion

## 4.1 Proximate analysis

The proximate analysis of Feedstock, RBC, and Fe-BC are tabulated in Table.1. The results showed that pyrolysis temperature affects the content of ash content, volatile matter, moisture content, and fixed carbon of feedstock and RBC. The moisture content of feedstock was 7.51% which reduces to 4.57% for RBC. The ash content of feedstock and RBC were 6.11% and 14.65% respectively. The ash content of RBC increased as pyrolysis temperature increased. This could because of higher degree of decomposition and mineral impurities (Hass & Lima, 2018). Similarly, the fixed carbon content of feedstock and RBC were 11.75% and 45.21% respectively. This increase in fixed carbon with pyrolysis temperature indicates the development of aromaticity (Hass & Lima, 2018)(Table 1).

Table 1: The proximate analysis of feedstock and RBC

| **Samples** | **Proximate Analysis** | | | |
|---|---|---|---|---|
| | **Moisture content (%)** | **Volatile matter (%)** | **Ash content (%)** | **Fixed carbon (%)** |
| **Feedstock** | 7.51 | 74.63 | 6.11 | 11.75 |
| **RBC** | 4.57 | 35.57 | 14.65 | 45.21 |

## 4.2 SEM analysis

Figure 7-10 (a, b) shows the SEM analysis of raw and Fe-BC. The SEM analysis identifies that the surface of the BC produced at a pyrolysis temperature of 500$^{o}$C was smooth and had multiple pores. However, after modification with $FeCl_3$, the BC surface becomes rough, and different irregular particles are attached to the surface, tells that the impregnation of Fe onto the surface and in the pores of BC was successful (Y. Wang et al., 2022a). These results are confirmed by EDS analysis.

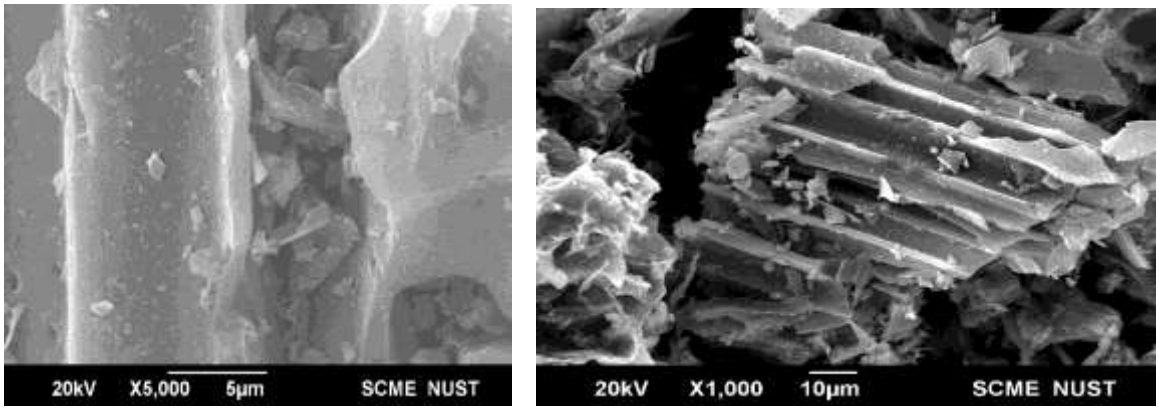


Figure 7:(a) and (b) displays images of raw bagasse biochar.

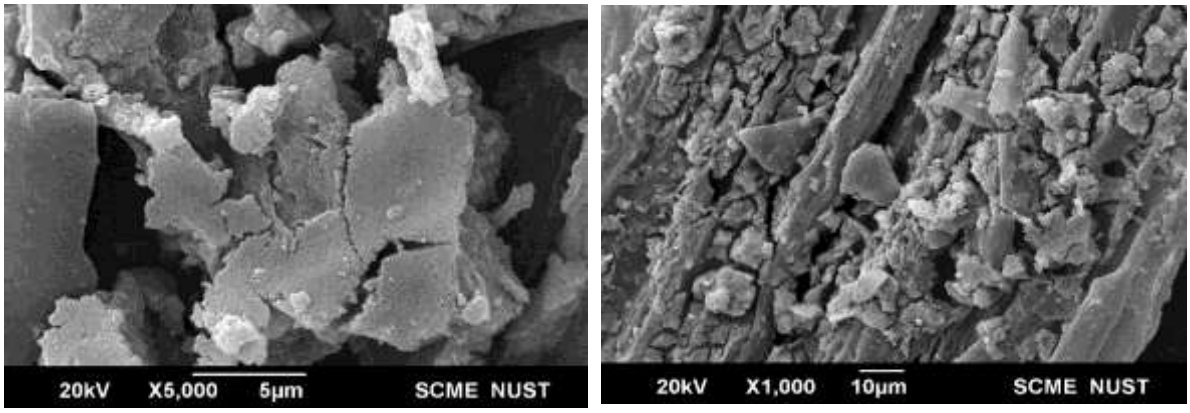


Figure 8:(a) and (b) displays SEM images of Fe-biochar.

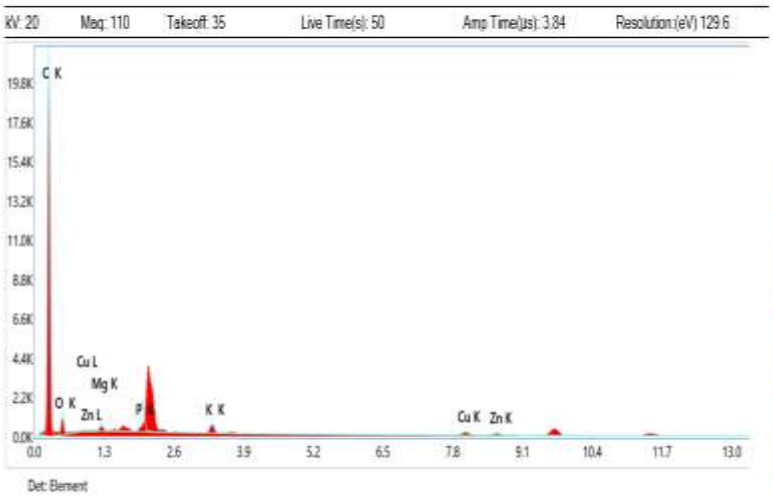


eZAF Quant Result - Analysis Uncertainty: 14.48 %

| Element | Weight % | MDL | Atomic % | Error % |
|---|---|---|---|---|
| C K | 77.1 | 1.02 | 85.9 | 10.0 |
| O K | 13.0 | 0.30 | 10.9 | 12.6 |
| Mg K | 0.8 | 0.09 | 0.5 | 10.8 |
| P K | 3.0 | 0.08 | 1.3 | 3.7 |
| K K | 1.4 | 0.10 | 0.5 | 5.3 |
| Cu K | 2.5 | 0.29 | 0.5 | 9.0 |
| Zn K | 2.2 | 0.35 | 0.4 | 4.8 |

Figures 9(a) and (b) displays EDS analysis of raw biochar.

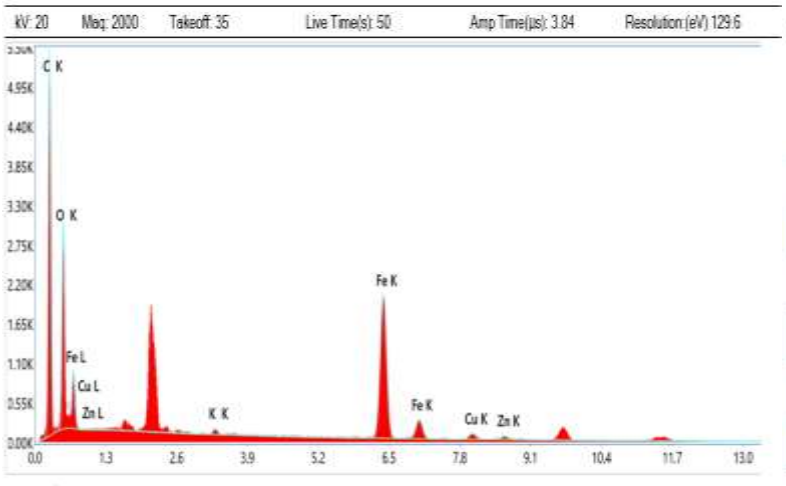


eZAF Quant Result - Analysis Uncertainty: 11.29 %

| Element | Weight % | MDL | Atomic % | Error % |
|---|---|---|---|---|
| C K | 40.7 | 1.32 | 59.7 | 11.0 |
| O K | 27.6 | 0.37 | 30.4 | 10.8 |
| K K | 0.4 | 0.13 | 0.2 | 18.0 |
| Fe K | 27.4 | 0.28 | 8.6 | 2.5 |
| Cu K | 2.2 | 0.42 | 0.6 | 16.7 |
| Zn K | 1.6 | 0.50 | 0.4 | 6.6 |

Figures 10(a) and (b) displays the EDS analysis of Fe-biochar.

## 4.3 FTIR

The FTIR analysis technique was applied to explore the functional groups that are present on the surface of unmodified and modified BC before and after the adsorption experiments are done. The results are displayed in Figure 11. The broad FTIR absorbance peak of RBC ad Fe-BC at 3300 – 3600 $cm^{-1}$ was corresponding to the aldehydes and alcohols or -OH (Min et al., 2020b), demonstrating the existence of certain hydroxyl groups on the RBC and Fe-BC surfaces. The peaks present at 2850 and 2930 $cm^{-1}$ are attributable to the vibrations of aliphatic hydrocarbon and C-H and $-CH_2$ (Jinn et al., 2018). The distinctive peak at 1606 and 1608 $cm^{-1}$ appears due to Aromatic C-C groups or because of stretching vibration of C-O functional groups present in ketones, quinones, and amides (H. Wang et al., 2017). The presence of carboxylate groups (O=C-O) is shown by the peak that appeared at 1238 $cm^{-1}$ reference as displayed in Fig.11(a). The FTIR shows that the RBC had numerous functional groups of -OH, -COOH, and -C-O-C that are present on its surface, which present several effective locations to remove Cr (VI). Additionally, a new peak at 573$cm^{-1}$ was also observed for Fe-BC as shown in Figure 11(b) which corresponds to the formation of Fe-O stretch, demonstrating that $Fe_2O_3$ and $Fe_3O_4$ were impregnated onto the surface of BC. Results show that after modification, the intensity of peaks at 1809 and 849 has increased which showed that mass per unit volume of corresponding compounds have increased after modification. (Khan et al., 2015). After removal of Cr (VI) by RBC, and Fe-BC, the FTIR spectrum as shown in Figure 11(b) shows some observable changes like a new peak appeared at 2325. This may be

because of the formation of the complexion between functional groups present on BC surface and Cr (VI) in aqueous solution (Lin et al., 2018).

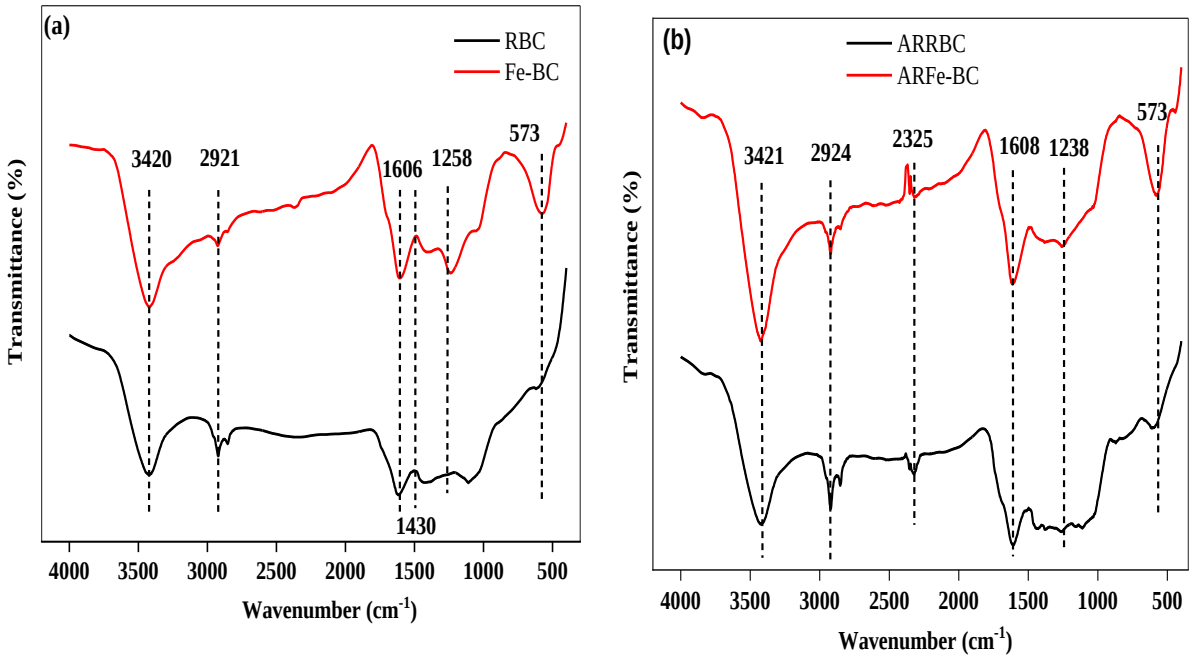


Figure 11: FTIR analysis of (a) RBC and Fe-BC before and (b) after Cr (VI) removal

## 4.4 BET analysis

The BET analysis results of RBC and Fe-BC samples are presented in Table.2. The RBC sample possess a BET surface area of 31.63 $m^2/g$ and has a total pore volume of 0.054 $cm^3/g$. Whereas, the BET surface area and total pore volume in the case of Fe-BC are 27.18 $m^2/g$ and 0.027$cm^3/g$ respectively. The reduction in BET surface area and pore volume after modification with $FeCl_3$ could be because of the loading of iron oxide particles on the surface of RBC which ultimately blocked the pores. Same results were also presented by Yi et al.2021 (Yi et al., 2021b). These results are consistent with the SEM analysis.

Table 2:Textural properties of RBC and Fe-BC

| Samples | $S_{BET}$ ($m^2/g$) | Pore volume ($cm^3/g$) | Pore width (nm) |
|---|---|---|---|
| RBC | 31.63 | 0.054 | 1.731 |
| Fe-BC | 27.18 | 0.027 | 1.214 |

## 4.5 Point of zero charge (PZC)

The pH at which surface charge on biochar surface is zero is called the point of zero charge (PZC). The raw BC in this work presents neutral to slightly basic pH values (7.72 ±0.2). After modification with $FeCl_3$, the adsorbent shows a PZC value of (7.5 ± 0.2). High PZC value for RBC and Fe-BC as displayed in Figure 12 (a) and (b) respectively suggests that the basic functional groups dominate on their surfaces (Herath et al., 2021a). The washing step after modification removes some of the ash content which results in decreasing the PZC for Fe-BC to 7.5 ± 0.2. These findings are matched with the results of Dias et. 2020 (Dias et al., 2020).

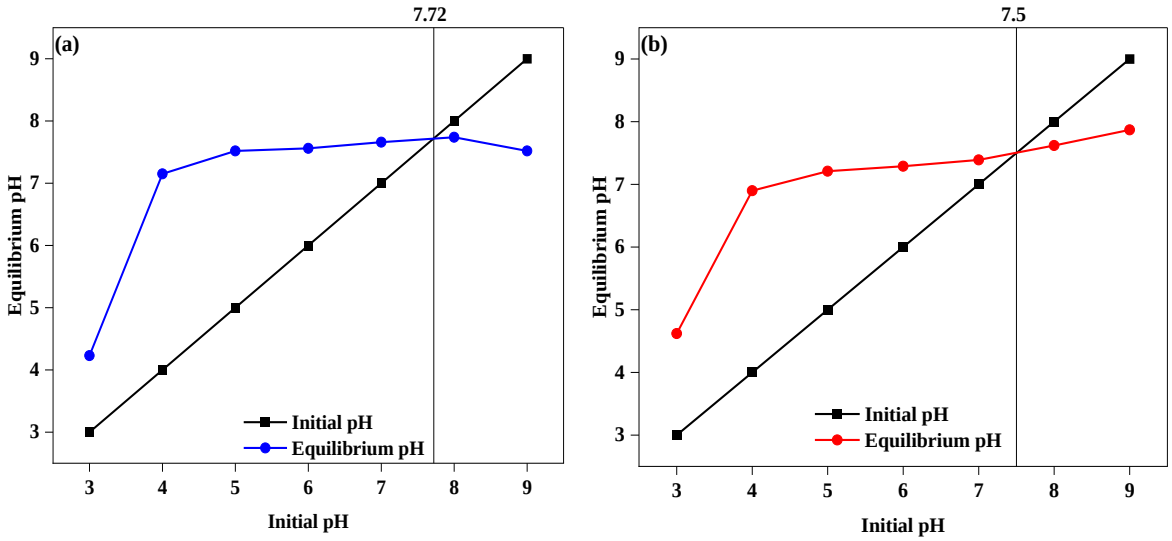


Figure 12: Point of zero charge (PZC) of (a) RBC (b) Fe-BC.

# 4.6 Adsorption results

## 4.6.1 Selection of suitable biochar

To select the most suitable BC for modification and eventually for the elimination of Cr (VI) from water, adsorbent dosage experiments were conducted. Three BC samples were prepared at three distinctive temperatures i.e., 400°C, 500°C, and 600°C and experiments were conducted for the adsorbent dosage of 1-5 g/L. Figure 13 depicts that the removal percentage enhances with the enhance in adsorbent dosage and is maximum for BC prepared at the temperature of 500°C. Thus, the BC prepared at 500°C was selected for modification with $FeCl_3$ and further removal experiments of Cr (VI).

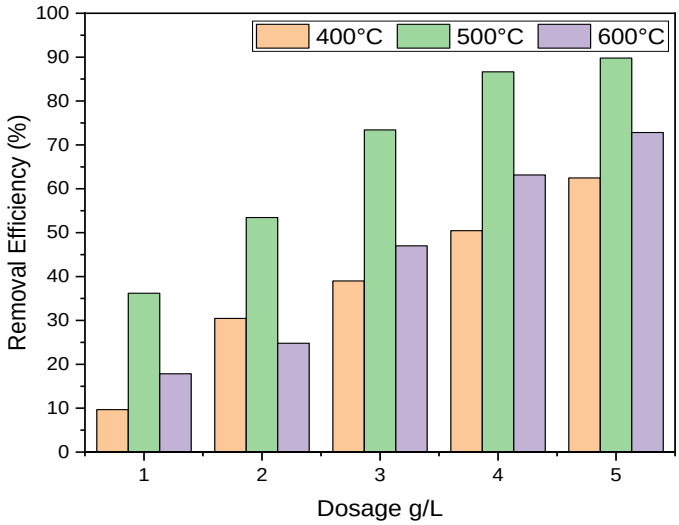


Figure 13: Selection of suitable biochar (RBC) for modification and removal of Cr (VI)

### 4.6.2 Effect of adsorbent dosage

Figure 14 illustrates how the dosage of RBC and Fe-BC affected the effectiveness of the elimination and adsorption of Cr (VI). When the adsorbent dose rose from 1 g/L to 5 g/L, the elimination efficiency for RBC improved from 36.19% to 89.78%. Similarly, the removal efficiency increased from 63.86% to 100% as displayed in Figure 14(b) with the enhance in adsorbent dosage of Fe-BC from 1 g/L to 5 g/L. The elimination percentage enhanced rapidly when the adsorbent dose increased from 1 to 3 g/L as compared to 3 to 5 g/L for both absorbents, however the efficiency is higher for Fe-BC. This could be because of the existence of Fe ions that are impregnated on the surface of Fe-BC as can be identified from the SEM and FTIR results in sections 4.2 and 4.3 respectively. Moreover, the adsorption capacity showed reduction for both adsorbents as adsorbent dosage enhances. The gradient of Cr (VI) concentration between sorbate and adsorbent fell, which results in a reduction in Cr (VI) adsorption capacity (Pellera et al., 2012). 3 g/L of the adsorbent dosage was found to be ideal in terms of removal effectiveness and cost-benefit and was employed in future studies.

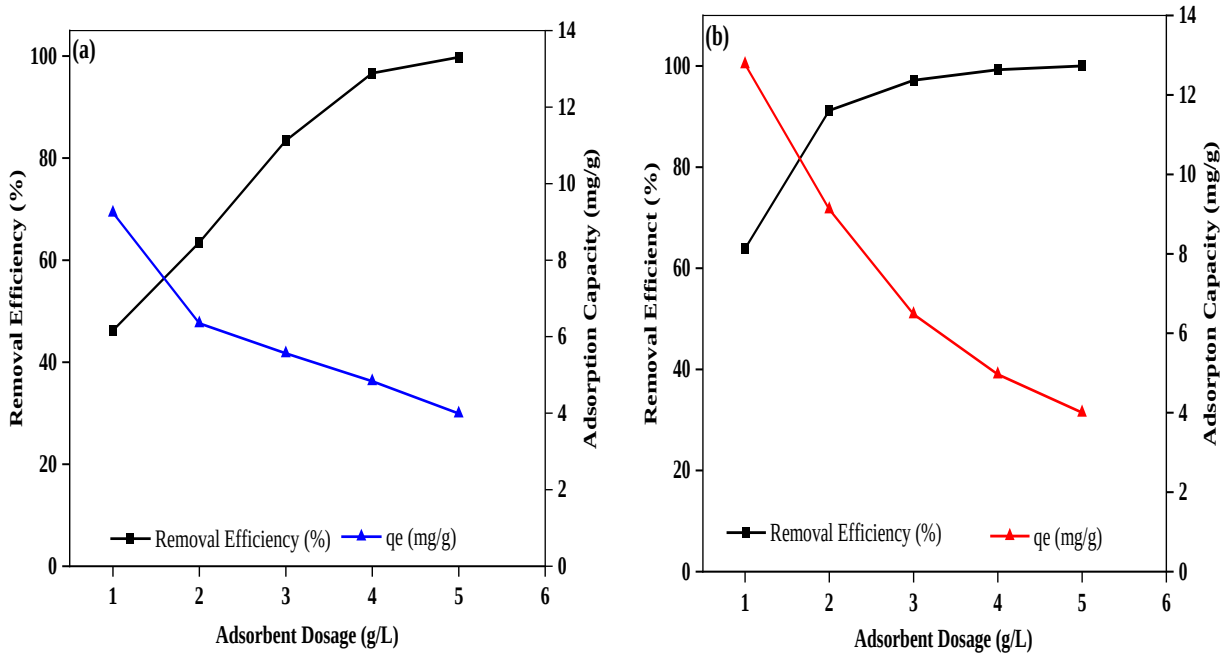


Figure 14: Impact of adsorbent dose on the elimination percentage (%) and adsorption capacity (mg/g) of (a) RBC and (b) Fe-BC.

### 4.6.3 pH effect

To identify ideal pH, the impact of pH on the reaction of adsorption of Cr (VI) from RBC and Fe-BC was investigated between the range of pH 2 to 10. The results are depicted in Figure 15. All other parameters i.e., Adsorbent dosage, temperature, contact time, and initial concentration of Cr (VI) were kept constant. The removal efficiency was 73.82% and 92.65% for RBC and Fe-BC at pH 2 respectively. Similarly, the adsorption capacity of Fe-BC reached 6.18 mg/g as compared to 4.92 mg/g for RBC. The increase in removal efficiency and adsorption capacity for Fe-BC because of the impregnation of iron particles on the surface as shown in the FTIR results in section 4.3. Chromium occurs as $HCrO_4^-$, $Cr_2O_7^{2-}$ at pH less than 6 and as chromate ion ($CrO_4^{2-}$) at pH above 6. PZC of RBC and Fe-BC was 7.72 and 7.5 respectively as depicted in Figure 12(a, b) demonstrating that the adsorbent has positive charge when the pH of the solution is below than the PZC value i.e., (7.72 and 7.5) and negatively charged as pH value goes beyond PZC value (Jain et al., 2018a). When the pH of the solution is less than PZC, the positive charge appears on the adsorbent surface and contributes to eliminating the negatively charged species of Cr i.e., $HCrO_4^-$, $Cr_2O_7^{2-}$ . The conflict between chromate ($CrO_4^{2-}$) and hydroxyl ions ($OH^-$) for the adsorption surface of the adsorbent may, however, be the reason of the reduction in removal at

higher pH (Sun et al., 2021). Thus, to avoid the addition of chemicals for pH adjustment and for better removal efficiencies, The ideal pH was determined to be pH 2 which was selected for subsequent experiments.

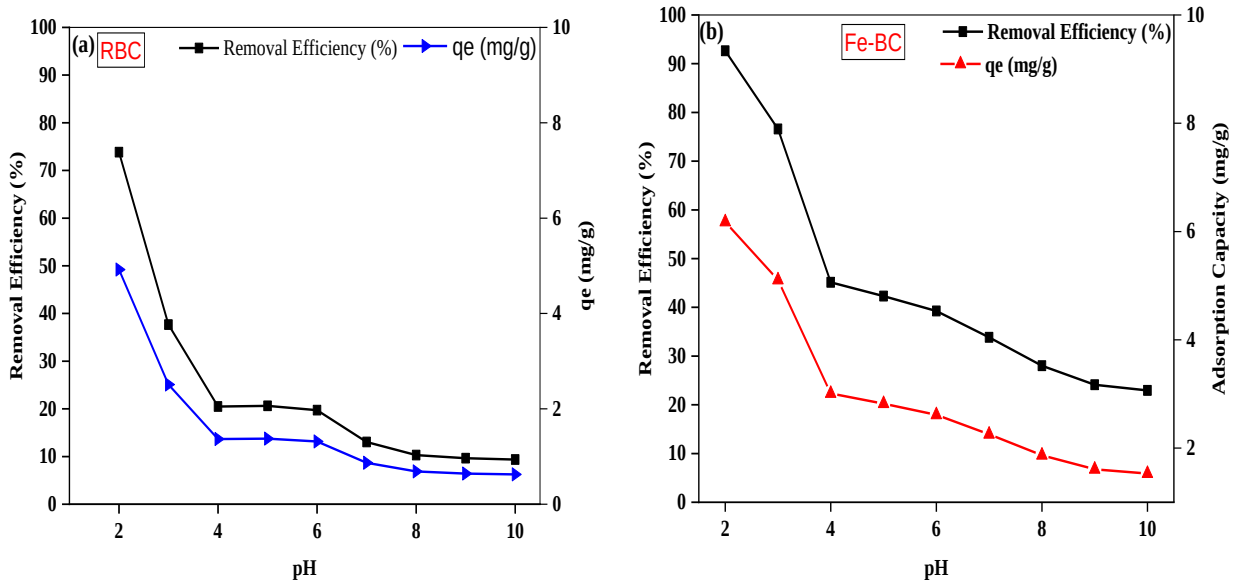


Figure 15:Impact of pH on the elimination efficiency (%) and adsorption capacity (mg/g) of (a) RBC and (b) Fe-BC.

### 4.6.4 Adsorption kinetics

The findings of the investigation into the impact of contact duration on effectiveness of Cr (VI) removal and adsorption capacity by RBC and Fe-BC are depicted in Figure 16. The contact time ranged from 0 to 180 minutes with an interval of 10 minutes. The other parameters were kept constant i.e., starting Cr (VI) concentration 20 mg/L, adsorbent dose 3 g/L, and pH 2. The results have shown that RBC removed more than 50% Cr (VI) from the solution during the first 60 minutes similarly in the meantime Fe-BC removed above 95% of the Cr (VI). High elimination percentage during the first 60 minutes. This could be because of the presence of more reaction sites on the surface of RBC and Fe-BC. However, as the contact time exceeds 60 minutes the process of Cr (VI) removal tends to decrease and reach equilibrium after 120 minutes for RBC. Further, an enhancement in contact time did not have any prominent effect on the removal efficiency of Cr (VI) and 120 minutes were chosen as the optimum time.

Moreover, pseudo-first order and pseudo-second-order kinetic models were implied to assess the experimental data; the findings are depicted in Figure 16. The obtained parameters from the

experimental data are presented in Table.3. The pseudo-second-order kinetic model better fits for both RBC and Fe-BC with regression co-efficient $R^2$ of 0.997 and 0.996 respectively as compared to pseudo-first-order kinetic model. This suggests that the rate-limiting step for the elimination of Cr (VI) was chemisorption and sharing or exchange of electrons between RBC, Fe-BC, and Cr (VI) are involved in the removal process.

Table 3: Parameters of adsorption kinetics

| | | Pseudo-first order Model | | | Pseudo-second order Model | | |
|---|---|---|---|---|---|---|---|
| Adsorbents | $q_e$, exp. (mg/g) | $q_e$, cal. (mg/g) | $K_1$ ($Min^{-1}$) | $R^2$ | $q_e$, cal (mg/g) | $K_2$ (g $mg^{-1}$ $min^{-1}$) | $R^2$ |
| RBC | 5.52 | 5.82 | 0.019 | 0.997 | 7.52 | 0.0024 | 0.995 |
| Fe-BC | 6.49 | 6.42 | 0.220 | 0.987 | 6.56 | 0.093 | 0.996 |

$q_e$, exp. – $q_e$, experimental; $q_e$, cal. – $q_e$, calculated

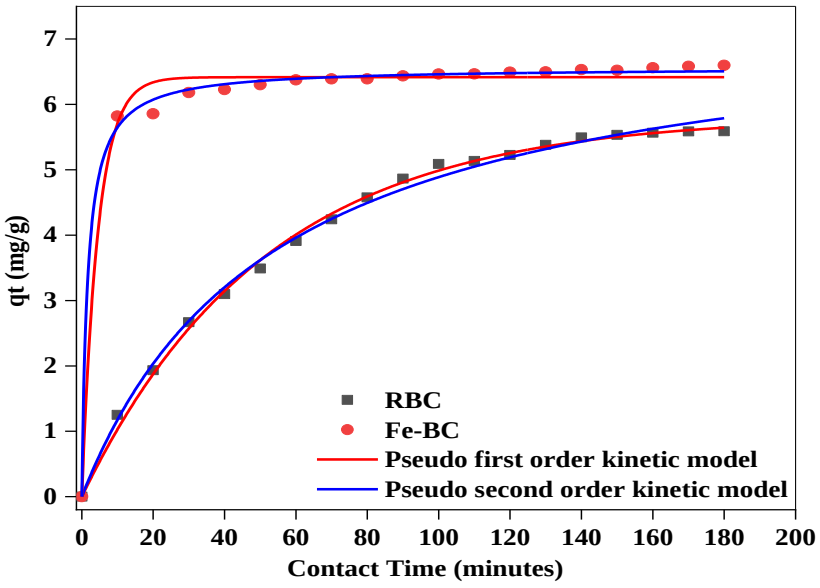


Figure 16: Adsorption kinetic fitted plots of (a) RBC and (b) Fe-BC.

### 4.6.5 Impact of initial concentration

In Figure 17, the impact of the starting Cr (VI) concentration on the elimination of Cr (VI) was investigated in range of 10 to 100 mg/L. The removal efficiencies of Cr (VI) are seen to decline as the starting concentration enhances. The elimination efficiency of RBC and Fe-BC decreased from 96.85% and 97.54% to 9.04% and 67.22% for initial concentration of 10mg/L to 100mg/L respectively. This is because of fewer active sites accessible and more intra-particle diffusion, the removal % showed reduction as the initial Cr (VI) concentrations increased (H. Wang et al., 2019). To increase elimination percentage, more adsorbents were required to keep balance of adequate ratio of adsorbate to adsorbent at high starting concentrations (de Paula et al., 2008). During the next studies, Cr (VI) at its ideal starting concentration of 20 mg/L was chosen due to its outstanding Cr (VI) adsorption capability.

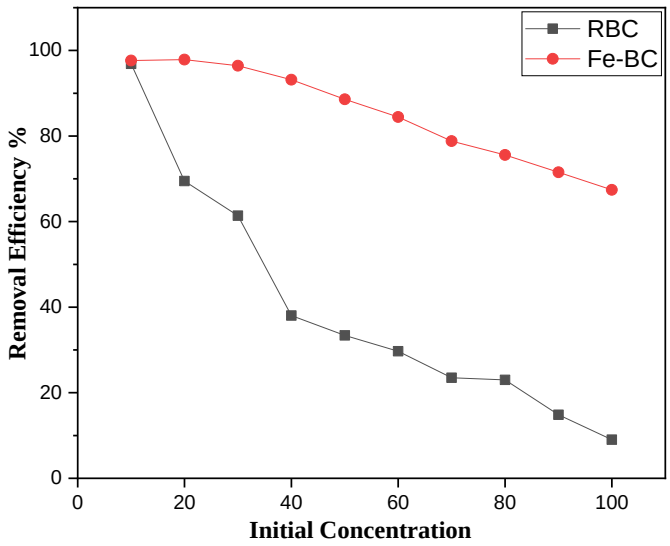


Figure 17: Impact of starting concentration on the elimination percentage (%) of RBC and Fe-BC

### 4.6.6 Adsorption isotherms

The creation of layers, the surface of the adsorbent, and the general mechanism of adsorption are all described by the adsorption isotherms model (Y. Wang et al., 2022b). In this work, the experimental data of initial Cr (VI) concentration ranging from 10 mg/L to 100 mg/L were used for Langmuir isotherm and Freundlich isotherm adsorption isotherm models. The fitted results are displayed in Figure 19 and the other parameters are displayed in Table. 3. The correlation co-efficient $R^2$ of Freundlich Isotherm is 0.99 and 0.97 for RBC and Fe-BC respectively as compared to the Langmuir Isotherm i.e., 0.93 and 0.93. The results depict that the Freundlich

Isotherm model better explains the adsorption behavior of Cr (VI) onto the surface of RBC and Fe-BC (Figure 18). This shows that the elimination of Cr (VI) by RBC and Fe-BC is governed through multilayer adsorption process (Shan et al., 2020). Additionally, the lower value of 1/n of Fe-BC indicates that Fe-BC had the greatest adsorption affinity for removal towards Cr (VI) in comparison with RBC (Yi et al., 2021c).

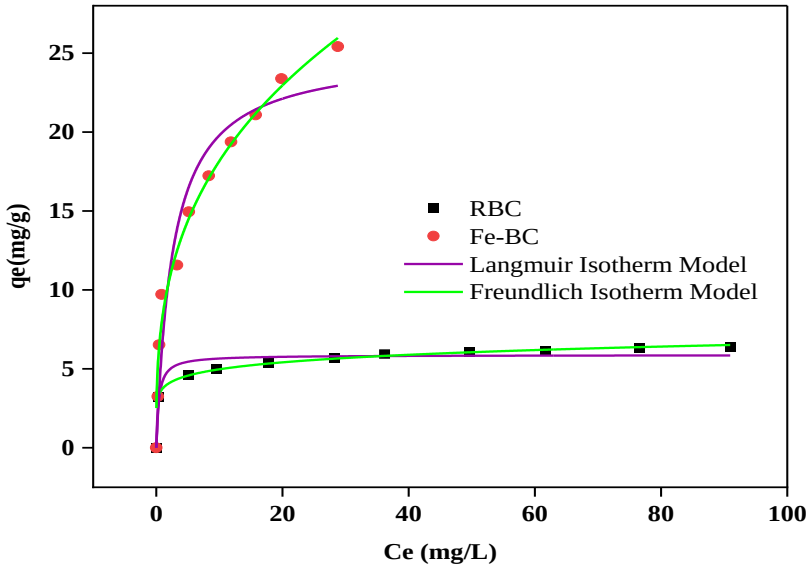


Figure 18: Adsorption isotherms fitted plots of (a) RBC and (b) Fe-BC

Table 4: Isotherm parameters for the adsorption of Cr (VI)

| Adsorbents | Langmuir parameters | | | Freundlich parameters | | |
|---|---|---|---|---|---|---|
| | $q_{max}$ (mg/g) | $K_L$ (L/mg) | $R^2$ | $1/n_F$ | $k_F$ (mg/g) $(L/mg)^{1/n}$ | $R^2$ |
| RBC | 5.86 | 2.55 | 0.93 | 0.12 | 3.75 | 0.99 |
| Fe-BC | 25.05 | 0.38 | 0.93 | 0.34 | 8.34 | 0.97 |

### 4.6.7 Effect of temperature

The elimination percentage of Cr (VI) is affected by variation in temperature. Removal experiments of Cr (VI) were performed by changing temperature value between 15ºC and 35ºC and the obtained results are depicted in Figure 19. For RBC, the elimination percentage at 15ºC was 63.64% while for Fe-BC, the removal efficiency was 83.08%. Similarly, at 35ºC the removal efficiency increased to 78.37% for RBC and 99.25% for Fe-BC. The findings demonstrated that, for RBC and Fe-BC, the increase in temperature favored elimination of Cr (VI) respectively. This phenomenon is primarily explained by the fact that a greater temperature enhances the rate of transfer of Cr (VI) by expanding the opportunities for interaction between Cr (VI) and RBC and Fe-BC, which eventually leads to a higher elimination percentage efficiency (Nassar, 2010). Moreover, the result shows that the reaction between adsorbent (RBC and Fe-BC) and Cr (VI) was an endothermic reaction in which rate of reaction increases with increase in temperature. (Jain et al., 2018b)

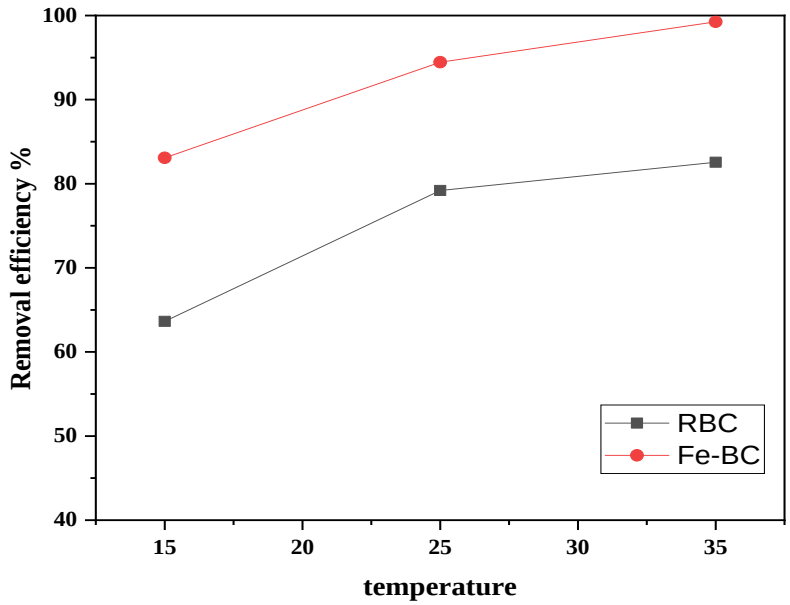


Figure 19: Effect of temperature

## 4.7 Interfering ions

Other than chromium ion, such as anions and cations are frequently present in the chromium-containing wastewater which battles with Chromium (VI) for adsorption sites present

on the surface of the adsorbent and lessen the efficiency of removal. Examples of these interfering ions are $CaCO_3$, $Na_2PO_4.12H_2O$, $Na_2SO_4$, $MgCl_2$, and Humic acid. The influence of coexisting ions on the elimination of Cr (VI) are displayed in Fig. 20. After a 30-minute reaction, the elimination percentage of Chromium (VI) by Fe-based adsorbent were all reduced to around 70%, showing that the co-existing cations had an impact on the process.

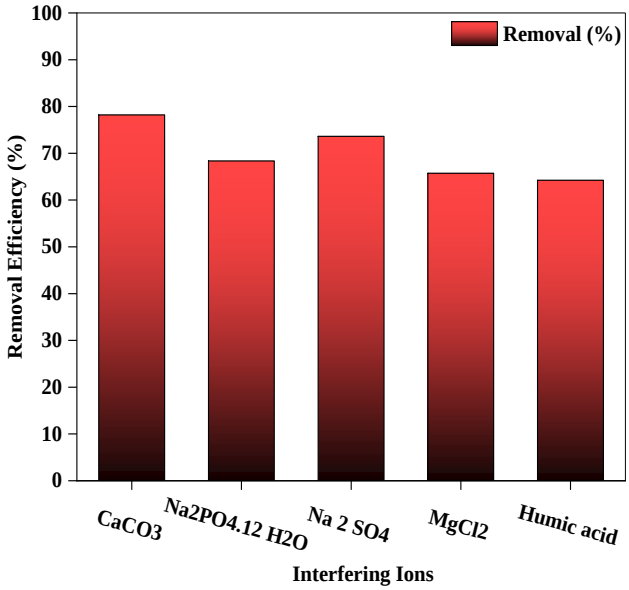


Figure 20: Impact of interfering ions

## 4.8 Regeneration experiment

The possibility of reuse of biochar material is a crucial requirement for effective and efficient practical use in wastewater treatment, indicating the system's re-generation efficiency and hence cost-effectiveness (Qin et al., 2022). Regeneration experiments were performed to analyze industrial application of Fe-based adsorbent for the elimination of Cr (VI). Several reusability experiments were performed, and the results are depicted in Figure 21. It was noted that the removal of Cr (VI) after the first three cycles was over 60% however after the fourth cycle it reduced to 49.31 %. These results of Cr (VI) removal after each cycle indicates that strong chemisorption occurs on the Fe-based adsorbent (Qin et al., 2022). Total use of surface functional groups or partial saturation of surface-active sites may also be reason for the steady decline in removal effectiveness of Chromium (VI) with each subsequent cycle (H. Guo et al., 2018). Thus,

the overall results portray Fe-based absorbent to be a useable adsorbent for the elimination of Cr (VI).

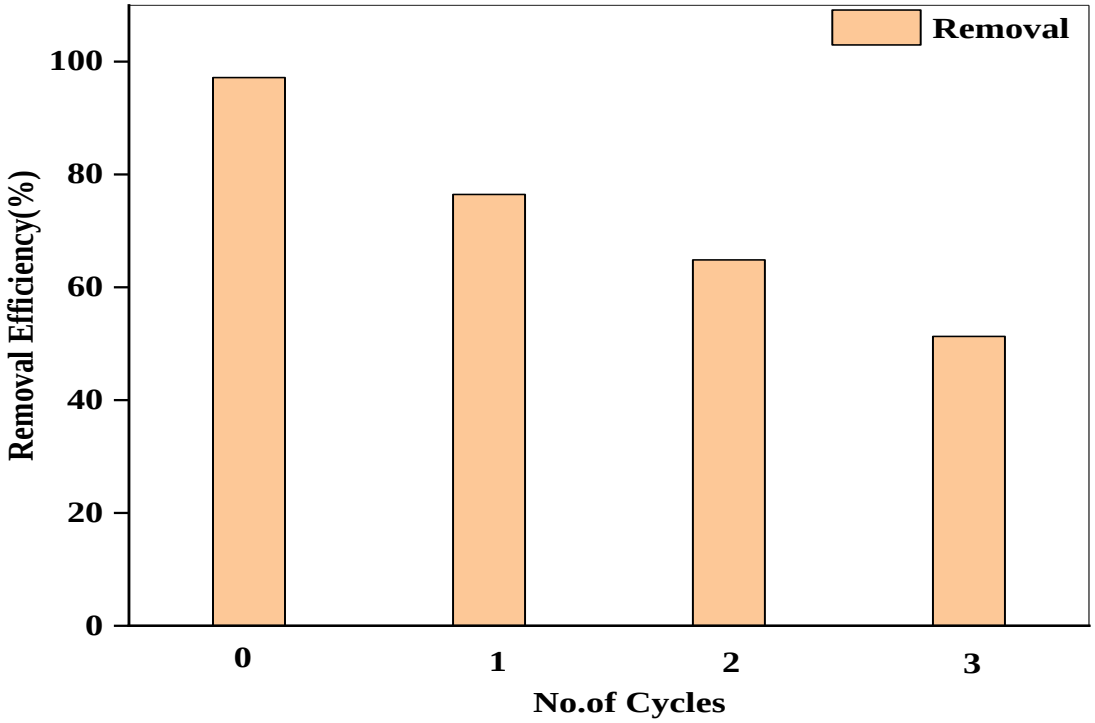


Figure 21:Impact of Regeneration cycle on removal Efficiency of Fe-BC

# Chapter 5

# Conclusion

## 5.1 Conclusion

The outcome of this study indicates that biochar prepared from sugarcane bagasse at temperature of 500°C is more efficient adsorbent than biochar prepared at temperature of 400°C and 600°C. the removal of Cr (VI) is probably due to the presence functional group present on the surface of biochar which forms complexion with Cr (VI) in the aqueous medium. the modification of RBC with $FeCl_3$ results in increase in removal efficiency of Cr (VI) which enhances the positive charge on the surface of biochar which attract the Cr (VI) by electrostatic force. The results indicate that the adsorption equilibrium was achieved within 120 minutes. Moreover, the experimental data of RBC better fitted the pseudo-first order kinetic model and the experimental data of Fe-BC better fitted the second order kinetic model. Both RBC and Fe-BC both followed Freundlich isotherm model. The greater Cr (VI) removal (92.65%) was achieved using 3 g/L Fe-BC at optimum pH (2), contact time (120 min) and initial Chromium (VI) concentration (20 mg/L) when compared with RBC (73.82% Cr (VI) removal). The maximum adsorption capacity ($q_{max}$) of Fe-BC for the elimination of Cr (VI) was 6.5 mg/g whereas, for RBC the $q_{max}$ was 4.92 mg/g. The regeneration experiment results showed the removal of Cr (VI) is maintained at over 50 % after the first three cycles which proved Fe-BC to be a promising adsorbent for the elimination of Cr (VI) for the water treatment.

## 5.2 Recommendations

For the future perspective, further studies should be focused in the following areas:

- removal of contaminants from the real wastewater
- Comparison with other feedstock material or combination should be explored
- Further work needs to be done to explore the removal mechanism of Cr (VI).

# References


Abbaci, F., Nait-Merzoug, A., Guellati, O., Harat, A., El Haskouri, J., Delhalle, J., Mekhalif, Z., & Guerioune, M. (2022). Bio/KOH ratio effect on activated biochar and their dye-based wastewater depollution. *Journal of Analytical and Applied Pyrolysis*, *162*, 105452.

https://doi.org/10.1016/j.jaap.2022.105452

Adam, M. R., Salleh, N. M., Othman, M. H. D., Matsuura, T., Ali, M. H., Puteh, M. H., Ismail, A. F., Rahman, M. A., & Jaafar, J. (2018). The adsorptive removal of chromium (VI) in aqueous solution by novel natural zeolite based hollow fiber ceramic membrane. *Journal of Environmental Management*, *224*, 252–262.

https://doi.org/10.1016/j.jenvman.2018.07.043

Aghababaei, A., Ncibi, M. C., & Sillanpää, M. (2017). Optimized removal of oxytetracycline and cadmium from contaminated waters using chemically activated and pyrolyzed biochar from forest and wood-processing residues. *Bioresource Technology*, *239*, 28–36.

https://doi.org/10.1016/j.biortech.2017.04.119

Ai, T., Jiang, X., Liu, Q., Lv, L., & Wu, H. (2019). Daptomycin adsorption on magnetic ultra-fine wood-based biochar from water: Kinetics, isotherms, and mechanism studies. BioresourceTechnology,273,8-15.

https://doi.org/10.1016/j.biortech.2018.10.039

Akter, S., Suhan, M. B. K., & Islam, M. S. (2022). Recent advances and perspective of electrocoagulation in the treatment of wastewater: A review. *Environmental Nanotechnology, Monitoring & Management*, *17*, 100643.

https://doi.org/10.1016/j.enmm.2022.100643

Albadarin, A. B., Mangwandi, C., Al-Muhtaseb, A. H., Walker, G. M., Allen, S. J., & Ahmad, M. N. M. (2012). Kinetic and thermodynamics of chromium ions adsorption onto low-cost dolomite adsorbent. *Chemical Engineering Journal*, *179*, 193–202.

https://doi.org/https://doi.org/10.1016/j.cej.2011.10.080

Babu, A. R., Yusub, S., Teja, P. M. V., Rao, P. S., Aruna, V., & Rao, D. K. (2019). Effect of Cr2O3 on the structural, optical, and dielectric studies of LiF-SrO-B2O3 glasses. *Journal of Non-Crystalline Solids*, *520*, 119428.

https://doi.org/https://doi.org/10.1016/j.jnoncrysol.2019.05.004

Bashir, S., Hussain, Q., Akmal, M., Riaz, M., Hu, H., Ijaz, S. S., Iqbal, M., Abro, S., Mehmood, S., & Ahmad, M. (2018). Sugarcane bagasse-derived biochar reduces the cadmium and chromium bioavailability to mash bean and enhances the microbial activity in contaminated soil. *Journal of Soils and Sediments*, *18*(3), 874–886.

https://doi.org/10.1007/s11368-017-1796-z

Bayazit, Ş. S., & Kerkez, Ö. (2014). Hexavalent chromium adsorption on superparamagnetic multi-wall carbon nanotubes and activated carbon composites. *Chemical Engineering Research and Design*,*92*(11), 2725–2733.

https://doi.org/10.1016/j.cherd.2014.02.007

Bohdziewicz, J. (2000). Removal of chromium ions (VI) from underground water in the hybrid complexation-ultrafiltration process. *Desalination*, *129*(3), 227–235.

https://doi.org/https://doi.org/10.1016/S0011-9164(00)00063-1

Chen, B., Chen, Z., & Lv, S. (2011). A novel magnetic biochar efficiently sorbs organic pollutants and phosphate. *Bioresource Technology*, *102*(2), 716–723. https://doi.org/10.1016/j.biortech.2010.08.067

Chen, B., Chen, Z., & Lv, S. (2011). A novel magnetic biochar efficiently sorbs organic pollutants and phosphate. Bioresources Technology, 102(2), 716-723.

https://doi.org/10.1016/j.biortech.2010.08.067

Chen, T., Zhou, Z., Xu, S., Wang, H., & Lu, W. (2015). Adsorption behavior comparison of trivalent and hexavalent chromium on biochar derived from municipal sludge. *Bioresource Technology*, *190*, 388–394.

https://doi.org/10.1016/j.biortech.2015.04.115

Costa, M. (2003). Potential hazards of hexavalent chromate in our drinking water. *Toxicology and Applied Pharmacology*, *188*(1), 1–5.

https://doi.org/10.1016/S0041-008X(03)00011-5

Danish, M., & Ahmad, T. (2018). A review on utilization of wood biomass as a sustainable precursor for activated carbon production and application. *Renewable and Sustainable Energy Reviews*, *87*, 1–21.

https://doi.org/10.1016/j.rser.2018.02.003

de Paula, H. A., Becker, J. G., & Davis, A. P. (2008). Characterization of the Uptake of Divalent Metal Ions by a Hatchery Residual. *Environmental Engineering Science*, *25*(5), 737–746.

https://doi.org/10.1089/ees.2007.0141

Di Stasi, C., Alvira, D., Greco, G., González, B., & Manyà, J. J. (2019). Physically activated wheat straw-derived biochar for biomass pyrolysis vapors upgrading with high resistance against coke deactivation fuel, 255, 115807.

https://doi.org/10.1016/j.fuel.2019.115807

Dias, D., Bernardo, M., Matos, I., Fonseca, I., Pinto, F., & Lapa, N. (2020). Activation of co-pyrolysis chars from rice wastes to improve the removal of Cr3+ from simulated and real industrial wastewaters. *Journal of cleaner production*, 267.

https://doi.org/10.1016/j.jclepro.2020.121993

Doke, S. M., & Yadav, G. D. (2014). Process efficacy and novelty of titania membrane prepared by polymeric sol–gel method in removal of chromium (VI) by surfactant enhanced microfiltration. *Chemical Engineering Journal*, 255, 483-491.

https://doi.org/10.1016/j.cej.2014.05.098

Dong, X., Ma, L. Q., & Li, Y. (2011). Characteristics and mechanisms of hexavalent chromium removal by biochar from sugar beet tailing. *Journal of Hazardous Materials*, *190*(1–3), 909–915.

https://doi.org/10.1016/j.jhazmat.2011.04.008

Fahmy, Y., Fahmy, T. Y. A., Mobarak, F., El-Sakhawy, M., & Fadl, M. H. (2017). Agricultural Residues (Wastes) for Manufacture of Paper, Board, and Miscellaneous Products: Background Overview and Future Prospects. *International Journal of ChemTech Research*, *10*(2), 424–448.

https://doi.org/10.5281/zenodo.546735

Farooq, M. Z., Zeeshan, M., Iqbal, S., Ahmed, N., & Shah, S. A. Y. (2018). Influence of waste tire addition on wheat straw pyrolysis yield and oil quality. *Energy*, *144*, 200–206.

https://doi.org/10.1016/j.energy.2017.12.026

Gaikwad, M. S., & Balomajumder, C. (2017). Simultaneous rejection of chromium(VI) and fluoride [Cr(VI) and F] by nanofiltration: Membranes characterizations and estimations of membrane transport parameters by CFSK model. *Journal of Environmental Chemical Engineering*, *5*(1), 45–53.

https://doi.org/https://doi.org/10.1016/j.jece.2016.11.018

Genawi, N. M., Ibrahim, M. H., El-Naas, M. H., & Alshaik, A. E. (2020). Chromium Removal from Tannery Wastewater by Electrocoagulation: Optimization and Sludge Characterization. In *Water* (Vol. 12, Issue 5).

https://doi.org/10.3390/w12051374

Godinho, D., Dias, D., Bernardo, M., Lapa, N., Fonseca, I., Lopes, H., & Pinto, F. (2017). Adding value to gasification and co-pyrolysis chars as removal agents of Cr3+. *Journal of Hazardous Materials*, *321*, 173–182.

https://doi.org/https://doi.org/10.1016/j.jhazmat.2016.09.006

Golder, A. K., Chanda, A. K., Samanta, A. N., & Ray, S. (2007). Removal of Cr(VI) from Aqueous Solution: Electrocoagulation vs Chemical Coagulation. *Separation Science and Technology*, *42*(10), 2177–2193.

https://doi.org/10.1080/01496390701446464

Government of Pakistan. (2021). *02-Agriculture Economic survey 2021*.

https://www.finance.gov.pk/survey/chapters_21/02-Agriculture.pdf

Grigore, M. E. (2017a). Methods of Recycling, Properties and Applications of Recycled Thermoplastic Polymers. In *Recycling* (Vol. 2, Issue 4).

https://doi.org/10.3390/recycling2040024

Grigore, M. E. (2017b). Methods of recycling, properties, and applications of recycled thermoplastic polymers. *Recycling*, *2*(4), 1–11.

https://doi.org/10.3390/recycling2040024

Guo, H., Bi, C., Zeng, C., Ma, W., Yan, L., Li, K., & Wei, K. (2018). Camellia oleifera seed shell carbon as an efficient renewable bio-adsorbent for the adsorption removal of hexavalent chromium and methylene blue from aqueous solution. *Journal of Molecular Liquids*, *249*, 629–636.

https://doi.org/10.1016/j.molliq.2017.11.096

Guo, W., Lu, S., Shi, J., & Zhao, X. (2019). Effect of corn straw biochar application to sediments on the adsorption of 17α-ethinyl estradiol and perfluorooctane sulfonate at sediment-water interface. *Ecotoxicology and Environmental Safety*, *174*, 363–369.

https://doi.org/10.1016/j.ecoenv.2019.01.128

Guo, X., Liu, A., Lu, J., Niu, X., Jiang, M., Ma, Y., Liu, X., & Li, M. (2020). Adsorption mechanism of hexavalent chromium on biochar: Kinetic, thermodynamic, and characterization studies. *ACS Omega*, *5*(42), 27323–27331.

https://doi.org/10.1021/acsomega.0c03652

Hamadi, N. K., Chen, X. D., Farid, M. M., & Lu, M. G. Q. (2001). Adsorption kinetics for the removal of chromium (VI) from aqueous solution by adsorbents derived from used tyres and sawdust. *Chemical Engineering Journal*, *84*(2), 95–105.

https://doi.org/10.1016/S1385-8947(01)00194-2

Hass, A., & Lima, I. M. (2018). Effect of feed source and pyrolysis conditions on properties and metal sorption by sugarcane biochar. *Environmental Technology and Innovation*, *10*, 16–26.

https://doi.org/10.1016/j.eti.2018.01.007

Hayashi, N., Matsumura, D., Hoshina, H., Ueki, Y., Tsuji, T., Chen, J., & Seko, N. (2021). Chromium (VI) adsorption–reduction using a fibrous amidoxime-grafted adsorbent. *Separation and Purification Technology*, *277*, 119536.

https://doi.org/10.1016/j.seppur.2021.119536

Herath, A., Layne, C. A., Perez, F., Hassan, E. B., Pittman, C. U., & Mlsna, T. E. (2021a). KOH-activated high surface area Douglas Fir biochar for adsorbing aqueous Cr (VI), Pb (II) and Cd(II). *Chemosphere*, *269*, 128409.

https://doi.org/10.1016/j.chemosphere.2020.128409

Herath, A., Layne, C. A., Perez, F., Hassan, E. I. B., Pittman, C. U., & Mlsna, T. E. (2021b). KOH-activated high surface area Douglas Fir biochar for adsorbing aqueous Cr (VI), Pb(II) and Cd(II). *Chemosphere*, *269*, 128409.

https://doi.org/10.1016/j.chemosphere.2020.128409

Ioannidou, O., & Zabaniotou, A. (2007). Agricultural residues as precursors for activated carbon production—A review. *Renewable and Sustainable Energy Reviews*, *11*(9), 1966–2005.

https://doi.org/10.1016/j.rser.2006.03.013

Jain, M., Yadav, M., Kohout, T., Lahtinen, M., Garg, V. K., & Sillanpää, M. (2018a). Development of iron oxide/activated carbon nanoparticle composite for the removal of Cr (VI), Cu (II) and Cd(II) ions from aqueous solution. *Water Resources and Industry*, *20*, 54–74.

https://doi.org/10.1016/j.wri.2018.10.001

Jain, M., Yadav, M., Kohout, T., Lahtinen, M., Garg, V. K., & Sillanpää, M. (2018b). Development of iron oxide/activated carbon nanoparticle composite for the removal of Cr (VI), Cu(II) and Cd(II) ions from aqueous solution. *Water Resources and Industry*, *20*(June), 54–74.

https://doi.org/10.1016/j.wri.2018.10.001

Jin, X., Liu, Y., Tan, J., Owens, G., & Chen, Z. (2018). Removal of Cr (VI) from aqueous solutions via reduction and absorption by green synthesized iron nanoparticles. *Journal of Cleaner Production*, *176*, 929–936.

https://doi.org/10.1016/j.jclepro.2017.12.026

Joseph, S., Kammann, C. I., Shepherd, J. G., Conte, P., Schmidt, H.-P., Hagemann, N., Rich, A. M., Marjo, C. E., Allen, J., Munroe, P., Mitchell, D. R. G., Donne, S., Spokas, K., & Graber, E. R. (2018). Microstructural and associated chemical changes during the composting of a high temperature biochar: Mechanisms for nitrate, phosphate and other nutrient retention and release. *Science of The Total Environment*, *618*, 1210–1223.

https://doi.org/10.1016/j.scitotenv.2017.09.200

Kanagaraj, G., & Elango, L. (2019). Chromium and fluoride contamination in groundwater around leather tanning industries in southern India: Implications from stable isotopic ratio δ53Cr/δ52Cr, geochemical and geostatistical modelling. *Chemosphere*, *220*, 943–953.

https://doi.org/10.1016/j.chemosphere.2018.12.105

Karimi-Maleh, H., Ayati, A., Ghanbari, S., Orooji, Y., Tanhaei, B., Karimi, F., Alizadeh, M., Rouhi, J., Fu, L., & Sillanpää, M. (2021). Recent advances in removal techniques of Cr(VI) toxic ion from aqueous solution: A comprehensive review. *Journal of Molecular Liquids*, *329*, 115062.

https://doi.org/10.1016/j.molliq.2020.115062

Khan, M. Y., Mangrich, A. S., Schultz, J., Grasel, F. S., Mattoso, N., & Mosca, D. H. (2015). Green chemistry preparation of superparamagnetic nanoparticles containing Fe3O4 cores in biochar. *Journal of Analytical and Applied Pyrolysis*, *116*, 42–48.

https://doi.org/10.1016/j.jaap.2015.10.008

Kumar, A., & Jena, H. M. (2017). Adsorption of Cr (VI) from aqueous solution by prepared high surface area activated carbon from Fox nutshell by chemical activation with H3PO4. *Journal of Environmental Chemical Engineering*, *5*(2), 2032–2041.

https://doi.org/10.1016/j.jece.2017.03.035

Kuppusamy, S., Thavamani, P., Megharaj, M., Venkateswarlu, K., Lee, Y. B., & Naidu, R. (2016). Potential of Melaleuca diosmifolia leaf as a low-cost adsorbent for hexavalent chromium removal from contaminated water bodies. *Process Safety and Environmental Protection*, *100*, 173–182.

https://doi.org/10.1016/j.psep.2016.01.009

Li, R., Wang, J. J., Zhang, Z., Awasthi, M. K., Du, D., Dang, P., Huang, Q., Zhang, Y., & Wang, L. (2018). Recovery of phosphate and dissolved organic matter from aqueous solution using a novel CaO-MgO hybrid carbon composite and its feasibility in phosphorus recycling. *Science of The Total Environment*, *642*, 526–536.

https://doi.org/10.1016/j.scitotenv.2018.06.092

Lin, J., Su, B., Sun, M., Chen, B., & Chen, Z. (2018). Biosynthesized iron oxide nanoparticles used for optimized removal of cadmium with response surface methodology. *Science of the Total Environment*, *627*, 314–321.

https://doi.org/10.1016/j.scitotenv.2018.01.170

Lunk, H. J. (2015). Discovery, properties and applications of chromium and its compounds. *ChemTexts*, *1*(1). https://doi.org/10.1007/s40828-015-0007-z

Ma, F., Zhao, B., & Diao, J. (2019). Synthesis of magnetic biochar derived from cotton stalks for the removal of Cr (VI) from aqueous solution. *Water Science and Technology*, *79*(11), 2106–2115.

https://doi.org/10.2166/wst.2019.208

Ma, H.-L., Zhang, Y., Hu, Q.-H., Yan, D., Yu, Z.-Z., & Zhai, M. (2012). Chemical reduction and removal of Cr(vi) from acidic aqueous solution by ethylenediamine-reduced graphene oxide. *Journal of Materials Chemistry*, *22*(13), 5914–5916.

https://doi.org/10.1039/C2JM00145D

Min, L., Zhongsheng, Z., Zhe, L., & Haitao, W. (2020a). Removal of nitrogen and phosphorus pollutants from water by $FeCl_3$ - impregnated biochar. *Ecological Engineering*, *149*(March), 105792.

https://doi.org/10.1016/j.ecoleng.2020.105792

Min, L., Zhongsheng, Z., Zhe, L., & Haitao, W. (2020b). Removal of nitrogen and phosphorus pollutants from water by FeCl3- impregnated biochar. *Ecological Engineering*, *149*.

https://doi.org/10.1016/j.ecoleng.2020.105792

Mohamed, A. A.-R., El-Houseiny, W., EL-Murr, A. E., Ebraheim, L. L. M., Ahmed, A. I., & El-Hakim, Y. M. A. (2020). Effect of hexavalent chromium exposure on the liver and kidney tissues related to the expression of CYP450 and GST genes of Oreochromis niloticus fish: Role of curcumin supplemented diet. *Ecotoxicology and Environmental Safety*, *188*, 109890.

https://doi.org/10.1016/j.ecoenv.2019.109890

Mohan, D., Sarswat, A., Ok, Y. S., & Pittman, C. U. (2014). Organic and inorganic contaminants removal from water with biochar, a renewable, low cost and sustainable adsorbent – A critical review. *Bioresource Technology*, *160*, 191–202.

https://doi.org/10.1016/j.biortech.2014.01.120

Mortazavian, S., An, H., Chun, D., & Moon, J. (2018). Activated carbon impregnated by zero-valent iron nanoparticles (AC/nZVI) optimized for simultaneous adsorption and reduction of aqueous hexavalent chromium: Material characterizations and kinetic studies. *Chemical Engineering Journal*, *353*, 781–795.

https://doi.org/10.1016/j.cej.2018.07.170

Nassar, N. N. (2010). Rapid removal and recovery of Pb(II) from wastewater by magnetic nano adsorbents. *Journal of Hazardous Materials*, *184*(1–3), 538–546.

https://doi.org/10.1016/j.jhazmat.2010.08.069

Nidheesh, P. V, Scaria, J., Babu, D. S., & Kumar, M. S. (2021). An overview on combined electrocoagulation-degradation processes for the effective treatment of water and wastewater. *Chemosphere*, *263*, 127907.

https://doi.org/10.1016/j.chemosphere.2020.127907

O'Connor, D., Peng, T., Li, G., Wang, S., Duan, L., Mulder, J., Cornelissen, G., Cheng, Z., Yang, S., & Hou, D. (2018). Sulfur-modified rice husk biochar: A green method for the remediation of mercury contaminated soil. *Science of The Total Environment*, *621*, 819–826.

https://doi.org/10.1016/j.scitotenv.2017.11.213

Pakade, V. E., Tavengwa, N. T., & Madikizela, L. M. (2019). Recent advances in hexavalent chromium removal from aqueous solutions by adsorptive methods. *RSC Advances*, *9*(45), 26142–26164.

https://doi.org/10.1039/C9RA05188K

Pellera, F. M., Giannis, A., Kalderis, D., Anastasiadou, K., Stegmann, R., Wang, J. Y., & Gidarakos, E. (2012). Adsorption of Cu (II) ions from aqueous solutions on biochars prepared from agricultural by-products. *Journal of Environmental Management*, *96*(1), 35–42.

https://doi.org/10.1016/j.jenvman.2011.10.010

Qin, Y., Chai, B., Wang, C., Yan, J., Fan, G., & Song, G. (2022). Removal of tetracycline onto KOH-activated biochar derived from rape straw: Affecting factors, mechanisms, and reusability inspection. *Colloids and Surfaces A: Physicochemical and Engineering Aspects*, *640*(November 2021), 128466.

https://doi.org/10.1016/j.colsurfa.2022.128466

Qu, J., Wang, Y., Tian, X., Jiang, Z., Deng, F., Tao, Y., Jiang, Q., Wang, L., & Zhang, Y. (2021). KOH-activated porous biochar with high specific surface area for adsorptive removal of chromium (VI) and naphthalene from water: Affecting factors, mechanisms, and reusability exploration. *Journal of Hazardous Materials*, *401*, 123292.

https://doi.org/10.1016/j.jhazmat.2020.123292

Rainey, T. J., & Covey, G. (2016). Pulp and paper production from sugarcane bagasse. *Sugarcane-Based Biofuels and Bioproducts*, *October 2017*, 259–280.

https://doi.org/10.1002/9781118719862.ch10

Rizwan, M., Ali, S., Abbas, T., Adrees, M., Zia-ur-Rehman, M., Ibrahim, M., Abbas, F., Qayyum, M. F., & Nawaz, R. (2018). Residual effects of biochar on growth, photosynthesis

and cadmium uptake in rice (Oryza sativa L.) under Cd stress with different water conditions. *Journal of Environmental Management*, *206*, 676–683.

https://doi.org/10.1016/j.jenvman.2017.10.035

Saeed, MA, Irshad, A, Sattar, H. et al. (2015). *This is an author produced version of Agricultural Waste Biomass Energy Potential In White Rose Research Online URL for this paper : Saeed , MA , Irshad , A , Sattar , H et al .( 2015 ) Agricultural Waste Biomass Energy Potential In Pa*. 21–23.

Sanyal, T., Kaviraj, A., & Saha, S. (2015). Deposition of chromium in aquatic ecosystem from effluents of handloom textile industries in Ranaghat–Fulia region of West Bengal, India. *Journal of Advanced Research*, *6*(6), 995–1002.

https://doi.org/10.1016/j.jare.2014.12.002

Shaaban, A., Se, S.-M., Mitan, N. M. M., & Dimin, M. F. (2013). Characterization of Biochar Derived from Rubber Wood Sawdust through Slow Pyrolysis on Surface Porosities and Functional Groups. *Procedia Engineering*, *68*, 365–371.

https://doi.org/10.1016/j.proeng.2013.12.193

Shakya, A., & Agarwal, T. (2019). Removal of Cr(VI) from water using pineapple peel derived biochar: Adsorption potential and re-usability assessment. *Journal of Molecular Liquids*, *293*.

https://doi.org/10.1016/j.molliq.2019.111497

Shan, R., Shi, Y., Gu, J., Bi, J., Yuan, H., Luo, B., & Chen, Y. (2020). Aqueous Cr(VI) removal by biochar derived from waste mangosteen shells: Role of pyrolysis and modification on its absorption process. *Journal of Environmental Chemical Engineering*, *8*(4), 103885.

https://doi.org/10.1016/j.jece.2020.103885

Shen, Z., Hou, D., Zhao, B., Xu, W., Ok, Y. S., Bolan, N. S., & Alessi, D. S. (2018). Stability of heavy metals in soil washing residue with and without biochar addition under accelerated ageing. *Science of The Total Environment*, *619–620*, 185–193.

https://doi.org/10.1016/j.scitotenv.2017.11.038

Shi, Y., Shan, R., Lu, L., Yuan, H., Jiang, H., Zhang, Y., & Chen, Y. (2020). High-efficiency removal of Cr (VI) by modified biochar derived from glue residue. *Journal of Cleaner Production*, *254*, 119935.

https://doi.org/10.1016/j.jclepro.2019.119935

Silva, I. C. B. da, Basílio, J. J. N., Fernandes, L. A., Colen, F., Sampaio, R. A., & Frazão, L. A. (2017). Biochar from different residues on soil properties and common bean production. In *Scientia Agricola* (Vol. 74).

Sun, S., Zeng, X., Gao, Y., Zhang, W., Zhou, L., Zeng, X., Liu, W., Jiang, Q., Jiang, C., & Wang, S. (2021). Iron oxide loaded biochar/attapulgite composites derived camellia oleifera shells as a novel bio-adsorbent for highly efficient removal of Cr (VI). *Journal of Cleaner Production*, *317*.

https://doi.org/10.1016/j.jclepro.2021.128412

Szydłowski, W., & Łopatyński, J. (2003). Biological role of chromium. *Diabetologia Polska*, *10*, 365–370.

Tanhaei, B., Pourafshari Chenar, M., Saghatoleslami, N., Hesampour, M., Laakso, T., Kallioinen, M., Sillanpää, M., & Mänttäri, M. (2014). Simultaneous removal of aniline and nickel from water by micellar-enhanced ultrafiltration with different molecular weight cut-off membranes. *Separation and Purification Technology*, *124*, 26–35.

https://doi.org/10.1016/j.seppur.2014.01.009

Tytłak, A., Oleszczuk, P., & Dobrowolski, R. (2015). Sorption and desorption of Cr(VI) ions from water by biochar in different environmental conditions. *Environmental Science and Pollution Research*, *22*(8), 5985–5994.

https://doi.org/10.1007/s11356-014-3752-4

*UTILISING AGRICULTURAL WASTE TO ENHANCE FOOD SECURITY AND CONSERVE THE ENVIRONMENT*. (2011). *11*(6), 1–9.

Wang, B., Li, F., & Wang, L. (2020). Enhanced hexavalent chromium (Cr (VI)) removal from aqueous solution by Fe–Mn oxide-modified cattail biochar: adsorption characteristics and mechanism. *Chemistry and Ecology*, *36*(2), 138–154.

https://doi.org/10.1080/02757540.2019.1699537

Wang, H., Tian, Z., Jiang, L., Luo, W., Wei, Z., Li, S., Cui, J., & Wei, W. (2017). Highly efficient adsorption of Cr (VI) from aqueous solution by $Fe^{+3}$ impregnated biochar. *Journal of Dispersion Science and Technology*, *38*(6), 815–825.

https://doi.org/10.1080/01932691.2016.1203333

Wang, H., Zhang, M., & Lv, Q. (2019). Removal efficiency and mechanism of Cr (VI) from aqueous solution by maize straw biochar derived at different pyrolysis temperatures. *Water (Switzerland)*, *11*(4), 5–7.

https://doi.org/10.3390/w11040781

Wang, Y., Miao, J., Saleem, M., Yang, Y., & Zhang, Q. (2022a). Enhanced adsorptive removal of carbendazim from water by FeCl3-modified corn straw biochar as compared with pristine, HCl and NaOH modification. *Journal of Environmental Chemical Engineering*, *10*(1).

https://doi.org/10.1016/j.jece.2021.107024

Wang, Y., Miao, J., Saleem, M., Yang, Y., & Zhang, Q. (2022b). Enhanced adsorptive removal of carbendazim from water by FeCl3-modified corn straw biochar as compared with pristine, HCl and NaOH modification. *Journal of Environmental Chemical Engineering*, *10*(1), 107024.

https://doi.org/10.1016/j.jece.2021.107024

Wang, Z., Guo, H., Shen, F., Yang, G., Zhang, Y., Zeng, Y., Wang, L., Xiao, H., & Deng, S. (2015). Biochar produced from oak sawdust by Lanthanum (La)-involved pyrolysis for adsorption of ammonium ($NH_4^+$), nitrate ($NO_3^-$), and phosphate ($PO_4^{-3}$). *Chemosphere*, *119*, 646–653.

https://doi.org/10.1016/j.chemosphere.2014.07.084

Wei, X.-Z., Gan, Z.-Q., Shen, Y.-J., Qiu, Z.-L., Fang, L.-F., & Zhu, B.-K. (2019). Negatively charged nanofiltration membrane and its hexavalent chromium removal performance. *Journal of Colloid and Interface Science*, *553*, 475–483.

https://doi.org/https://doi.org/10.1016/j.jcis.2019.06.051

Wionczyk, B., Apostoluk, W., & Charewicz, W. A. (2006). Solvent extraction of chromium (III) from spent tanning liquors with Aliquat 336. *Hydrometallurgy*, *82*(1), 83–92.

https://doi.org/10.1016/j.hydromet.2006.03.055

Xia, D., Tan, F., Zhang, C., Jiang, X., Chen, Z., Li, H., Zheng, Y., Li, Q., & Wang, Y. (2016). ZnCl2-activated biochar from biogas residue facilitates aqueous As (III) removal. *Applied Surface Science*, *377*, 361–369.

https://doi.org/10.1016/j.apsusc.2016.03.109

Xia, P., Wang, X., Wang, X., Song, J., Wang, H., Zhang, J., & Zhao, J. (2016). Struvite crystallization combined adsorption of phosphate and ammonium from aqueous solutions by mesoporous MgO loaded diatomite. *Colloids and Surfaces A: Physicochemical and Engineering Aspects*, *506*, 220–227.

https://doi.org/https://doi.org/10.1016/j.colsurfa.2016.05.101

Yaashikaa, P. R., Senthil Kumar, P., Mohan Babu, V. P., Kanaka Durga, R., Manivasagan, V., Saranya, K., & Saravanan, A. (2019). Modelling on the removal of Cr(VI) ions from aquatic system using mixed biosorbent (Pseudomonas stutzeri and acid treated Banyan tree bark). *Journal of Molecular Liquids*, *276*, 362–370.

https://doi.org/https://doi.org/10.1016/j.molliq.2018.12.004

Yang, Q., Pan, X., Huang, F., & Li, K. (2010). Fabrication of High-Concentration and Stable Aqueous Suspensions of Graphene Nanosheets by Noncovalent Functionalization with Lignin and Cellulose Derivatives. *The Journal of Physical Chemistry C*, *114*(9), 3811–3816.

https://doi.org/10.1021/jp910232x

Yi, Y., Wang, X., Ma, J., & Ning, P. (2021a). Fe (III) modified Egeria najas driven-biochar for highly improved reduction and adsorption performance of Cr(VI). *Powder Technology*, *388*, 485–495.

https://doi.org/10.1016/j.powtec.2021.04.066

Yi, Y., Wang, X., Ma, J., & Ning, P. (2021b). Fe (III) modified Egeria najas driven-biochar for highly improved reduction and adsorption performance of Cr(VI). *Powder Technology*, *388*, 485–495.

https://doi.org/10.1016/j.powtec.2021.04.066

Yi, Y., Wang, X., Ma, J., & Ning, P. (2021c). Fe (III) modified Egeria najas driven-biochar for highly improved reduction and adsorption performance of Cr (VI). *Powder Technology*, *388*, 485–495.

https://doi.org/10.1016/j.powtec.2021.04.066

Yoon, J., Shim, E., Bae, S., & Joo, H. (2009). Application of immobilized nanotubular TiO2 electrode for photocatalytic hydrogen evolution: Reduction of hexavalent chromium (Cr(VI)) in water. *Journal of Hazardous Materials*, *161*(2), 1069–1074.

https://doi.org/https://doi.org/10.1016/j.jhazmat.2008.04.057

Zhang, Y., Ma, H.-L., Peng, J., Zhai, M., & Yu, Z.-Z. (2013). Cr (VI) removal from aqueous solution using chemically reduced and functionalized graphene oxide. *Journal of Materials Science*, *48*(5), 1883–1889.

https://doi.org/10.1007/s10853-012-6951-8

Zhou, L., Liu, Y., Liu, S., Yin, Y., Zeng, G., Tan, X., Hu, X., Hu, X., Jiang, L., Ding, Y., Liu, S., & Huang, X. (2016). Investigation of the adsorption-reduction mechanisms of hexavalent chromium by ramie biochars of different pyrolytic temperatures. *Bioresource Technology*, *218*, 351–359.

https://doi.org/10.1016/j.biortech.2016.06.102